Supplementary Materials for

Mfn2 agonists reverse mitochondrial defects in preclinical models of Charcot Marie Tooth disease type 2A

Agostinho G. Rocha[1#], Antonietta Franco[1#], Andrzej Krezel[2], Jeanne M. Rumsey[1], Justin M. Alberti[1], William C. Knight[1], Nikolaos Biris[3], Emmanouil Zacharioudakis[3], James W. Janetka[2], Robert H. Baloh[4], Richard N. Kitsis[5], Daria Mochly-Rosen[6], R. Reid Townsend[1], Evripidis Gavathiotis[3], Gerald W. Dorn II[1].

Correspondence to: gdorn@wustl.edu

This PDF file includes:

Materials and Methods
Figs. S1 to S31
Table S1
References 17 to 30

Other Supplementary Materials for this manuscript include:

Supplemental dataset 1 – NMR assignments, shift peaks, and constraints for Ser378 phosphorylated and unphosphorylated minipeptide studies.

Supplemental dataset 2 – Fusogenicity screening results, characteristics, and commercial sourcing of 55 candidate mitofusin agonists.

Supplemental dataset 3 – Characteristics and commercial sourcing of 12 (6 each) class A and class B mitofusin agonists.

Supplemental dataset 4 – Characteristics and sourcing of 4 novel newly synthesized chimeric classA/B mitofusin agonists.

Supplementary movies 1-4

Supplementary movie 1 – Hypothetical model of HR1 MP374-384 conformation before and after S378 phosphorylation.

Supplementary movie 2 – *In vitro* mouse mitochondrial mobility in Ctrl neuron, Mfn2 T105M neuron, and Mfn2 T105M neuron treated with compounds A+B (24 hours).

Supplementary movie 3 – Mitochondrial mobility in an axon of a control mouse sciatic nerve.

Supplementary movie 4 – Mitochondrial mobility in axons of a Mfn2 T105M mouse sciatic nerve before and at serial 20 minute periods after application of chimera B-A/l.

Materials and Methods
Cell lines and adenoviral constructs

Wild-type MEFs were prepared from E10.5 c57/bl6 mouse embryos. SV-40 T antigen-immortalized Mfn1 null (CRL-2992), Mfn2 null (CRL-2993) and Mfn1/Mfn2 double null MEFs (CRL-2994) (*17*) were purchased from ATCC. MEFs were subcultured in DMEM (4.5g/L glucose) plus 10% fetal bovine serum, 1× nonessential amino acids, 2 mM L-glutamine, 100U/ml penicillin and 100ug/ml streptomycin.

Human Mfn2 Ser378 was mutated to Ala or Asp by site-directed mutagenesis using the QuikChange Lightning kit (Agilent Technologies Inc.) and primers:

Mfn2-S378D-fw 5'-cgactcatcatggacgacctgcacatggcggc-3'
Mfn2-S378D-rv 5'-gccgccatgtgcaggtcgtccatgatgagtcg-3'
Mfn2-S378A-fw 5'-gactcatcatggacgccctgcacatggcg-3'
Mfn2-S378A-rv 5' –cgccatgtgcagggcgtccatgatgagtc-3'

Mfn2 and its mutants were sub-cloned into adenoviral vector Type 5 (dE1/E3) with RGD-fiber modification (Vector Biolabs) using BamHI/XhoI. All constructs were verified by Sanger DNA sequencing. Adeno-viral PINK1 was purchased from Vector Biolabs. Immunoblotting used mouse anti-Mfn2 (Abcam # ab56889, 1: 1000), anti-PINK1 (Sigma #P0076, 1: 500), and beta-actin (Santa Cruz Biotechnology #sc-81178, 1:1000). Protein detection and digital acquisition used peroxidase-conjugated anti mouse secondary antibody (Cell Signaling #7076S, 1:2500) and Western Lightning PLUS ECL substrate (Perkin Elmer 105001EA) on a Li-COR Odyssey instrument.

Peptide studies

The C-terminal and N-terminal Mfn2 367-384Gly peptides and Ala substituted variants of Mfn2 374-384 were chemically synthesized and introduced into cells using TAT47–57 conjugation (ThermoFisher Scientific). Except when indicated, 1 mM stocks in sterile water were diluted into culture media 1:1000 to achieve a final concentration of 1 μM. Cells were treated overnight.

For Alanine scanning the following peptides were synthesized:
(NH3) GI**A**DSLHMAARGGYGRKKRRQRRR (COOH)
(NH3) GIM**A**SLHMAARGGYGRKKRRQRRR (COOH)
(NH3) GIMD**A**LHMAARGGYGRKKRRQRRR (COOH)
(NH3) GIMDS**A**HMAARGGYGRKKRRQRRR (COOH)
(NH3) GIMDSL**A**MAARGGYGRKKRRQRRR (COOH)

The following peptides were synthesized for Ser378 substitution studies:
(NH3) GIMD**S**LHAAARGGYGRKKRRQRRR (COOH)
(NH3) GIMD**D**LHMAARGGYGRKKRRQRRR (COOH)
(NH3) GIMD**S(p)**LHMAARGGYGRKKRRQRRR (COOH)
(NH3) GIMD**G**LHMAARGGYGRKKRRQRRR (COOH)
(NH3) GIMD**C**LHMAARGGYGRKKRRQRRR (COOH)
(NH3) GIMD**N**LHMAARGGYGRKKRRQRRR (COOH)

Nuclear Magnetic Resonance (NMR) of HR1 peptide structure

Carboxyl terminal-amidated S378 parent and substituted peptide were synthesized for NMR studies:

Mfn2-371-384 (378S) – AVRGIMD**S**LHMAAR
Mfn2-371-384 (378S(p)) – AVRGIMD[**S(p)**]LHMAAR

Proton 2D NOESY and ^{15}N-^{1}H heteronuclear single quantum coherence overlay spectra of the above peptides were recorded on 600 MHz Bruker Avance III spectrometer equipped with cryoprobe, at 15 ˚C, pH 6, 50 mM NaCl, with each peptide at 2 mM concentration. Distance restraints were derived from observed NOE interactions between hydrogens within each peptide, and torsion angle restraints (φ and ψ) were derived from the observed chemical shifts (for C, H and N nuclei) (Supplemental dataset 1). The calculations used only experimental data; no theoretical molecular dynamics simulations/refinements were applied.

The helical structures/propensities in these peptides were not inferred or assumed from any single type of data. "Diagnostic" NOEs, in particular d_{NN} and $d_{ab}(i, i+3)$, were present in 200ms and 500ms mixing time H-H NOESY experiments, wherever signals could be resolved. The structural ensemble calculations used only restraints derived from NMR experiments. Distance restraints were derived from observed NOE interactions between hydrogens within each peptide, and torsion angle restraints (f and y) were derived from the observed chemical shifts (for C, H and N nuclei).

Both ensembles show preponderance of helical conformation between 378-383. These are more regular in phosphopeptide ensemble (fig. S5C). Both ensembles show no regular conformation between 371-376, consistent with a lack of observed NOEs and values of chemical shifts characteristic for unstructured sequences. At the current level of precision, there is little difference between two ensembles in positions of side chains for residues 379-383. The almost identical $^{13}C/^{1}H$ chemical shifts of these methyl groups also suggest the similarity of their positions and local environments. However, the backbone amide (N-H) and Ca signals clearly show differences, beyond the obvious one caused by phosphate esterification of serine. The amide signals shifted down-field (to higher values), a characteristic observed when amides form (or strengthen) hydrogen bonds within peptides. In general, the helical secondary structure is often stabilized by a negatively charged group "capping" the positive N-terminal end of the helix dipole. Here, a phosphorylation of Ser 378 can produce H-bonding for the amide of Leu-379 and the negative phosphate can additionally stabilize the helical turns following 379, providing an explanation for observed down-field shifts (i.e. H-bonding induced) in amides of 380, 381 and 382.

Mfn2 FRET for conformational studies

Mfn2 FRET probes contained N-termini-ceruleum and C-termini-mVenus fused to the human (h) mitofusin protein as described (*3*). FRET analyses were performed either on mitochondria isolated from Mfn1/Mfn2 null MEFs expressing the WT hMfn2 FRET-hMfn2 protein or intact Mfn1/Mfn2 null MEFs expressing WT or mutant Mfn2 FRET proteins (50 MOI). For isolated mitochondria studies 65 µg of organelle protein was used for each reaction in a total volume of 100 µl diluted in 10mM Tris-MOPS (pH 7.4), 10mM EGTA/Tris, 200mM sucrose. 1 µM of mitofusin agonist in DMSO was added simultaneously with 2µM mitofusin antagonist peptide, incubated in dark at room-temperature for 30 minutes, and FRET signal corrected for Cerulean signal analyzed using a Tecan Safire II multi-mode plate reader in polystyrene 96 well assay plate (Costar 3916). Data acquisition was: FRET – Excitation 433/8 nm, Emission 528/8 nm; Cerulean – Excitation 433/8 nm, Emission – 475/8 nm. Isolated mitochondria of non-infected cells were used to substract background, and FRET signals were normalized to respective cerulean signals. The % changes in FRET/Cerulean provoked by mitofusn antagonist peptide and reversed by different mitofusin agonist small molecules were compared to Mfn2-FRET mitochondria treated with water and DMSO, the vehicles for Mfn antagonist peptide and mitofusin agonist, respectively.

For FRET in intact cells, Mfn1/Mfn2 double null MEFs at 70% confluence were infected with adenoviri expressing FRET-hMfn2, FRET-hMfn2(S378A) or FRET hMfn2(S378D) at 50 MOI. Two-days after transduction and 1 hour after application of 1μM Mfn2 antagonist mini-peptide MP2 (*3*) to promote the closed/inactive Mfn conformation, cells were released from tissue culture substrate with trypsin/EDTA, washed, and transferred to a polystyrene 96 well assay plate (Costar 3916; 20,000 cells/50 μl/well). Fifty-microliters of modified Krebs-Henseleit buffer containing DMSO (vehicle) or 1 μM mitofusin agonist was added with gentle agitation for 10 min at room temperature. FRET and cerulean signals were assayed in a 96-well plate reader (TriStar 2S LB 942, Berthold Technologies) with 1 sec reading times at low sensitivity. Filters combinations are as follows: FRET – Excitation 430/10, Emission 535/25; Cerulean – Excitation 430/10, Emission – 475/20. Signals from non-infected cells were used for background correction. FRET was normalized to the respective cerulean signal for each well.

HR1 peptide-HR2 target binding assay

Target HR2 peptide sequence modified to include amino terminal 6 x His tags and Gly linkers, were bonded to Ni-NTA resin (4.4 μg/ml) (Quiagen) and used as immobilized "receptor" for amino-FITC-tagged Mfn2 374-384 (ligand) in which the Ser analogous to Ser378 was replaced with Asp to confer the negative charge essential for activity. FITC peptide ligands were suspended at 1 mM in 30% DMSO, 70% water (to minimize spontaneous aggregation) and diluted into binding buffer (de-ionized water). For the displacement binding, 2.5 nmol of FITC labeled agonist peptide was used in the presence or absence of different amounts of competing compounds. Resin-bound FITC signal (485 nm excitation/ 538 nm emission) measured in a 96 well spectrofluorometer (Spectramax M5e, Molecular Devices) represented binding to HR2 target. Competition binding isotherms were plotted and IC_{50} values calculated using Prism 7 (GraphPad).

Sequences for binding assay components are:

(NH3) HHHHHH-GGGG-AAMNKKIEVLDSLQSKAKLLRNKA-GG (COOH) (target)
(NH3) HHHHHH-GGGG-AAMNKKIEV**AA**S**A**QSKAKLLRNKA-GG (COOH) (target mutant)
(NH3) FITC-GGGG-AVRGIMD**S**LHMAAR-GG (COOH) (FITC labeled Ser peptide)
(NH3) FITC-GGGG-AVRGIMD**D**LHMAAR-GG (COOH) (FITC labeled Asp peptide)
(NH3) FITC-GGGG-AVRGIMD**A**LHMAAR-GG (COOH) (FITC labeled Ala peptide)

Protein and peptide modeling

The hypothetical structures of human Mfn2 were developed using the I-TASSER Suite package (*18*). The putative closed conformation is based on structural homology with bacterial dynamin-like protein (PDB: 2J69) (19), human Mfn1 (PDB:5GNS) (20), and *Arabidopsis thaliana* dynamin-related protein (PDB: 3T34) (21). The putative open conformation was based on structural homology with human Opa1, retrieved from the following structures: rat dynamin (PDB: 3ZVR) (22), human dynamin 1-like protein (PDB: 4BEJ) (23), and human myxovirus resistance protein 2 (PDB: 4WHJ) (24). Minipeptide and protein modeling used PEP-FOLD3 (http://bioserv.rpbs.univ-paris-diderot.fr/services/PEP-FOLD3/) and UCSF Chimera (*25*), respectively.

Protein alignment and phylogenetic analysis

Mfn2 orthologous sequences were retrieved from the Ensembl project database. Protein alignments were performed using Clustal Omega (*26*).

In vitro PINK1-Mfn2 phosphorylation assay

In silico prediction of kinases that might phosphorylate Mfn2 Ser378 in the peptide sequence AVRLIMD**S**LHMAARE used GPS 3.0 (http://gps.biocuckoo.org). GRK2/βARK1 was the top hit (score of 31.595), and GRK isoforms comprised 5 of the top 7 hits; ROCK kinase (score 15.919) and PKCα (score 11.48) were the other two hits. PINK1 kinase is not represented at this site, and no other sites reported any likely kinases for Mfn2 Ser378.

In vitro phosphorylation of Mfn2 by PINK1 and GRK kinases used a modified published protocol (*27*). Briefly, 20 μg of recombinant human Mfn2 (expressed in HEK293 cells; OriGene: TP326143) plus 10-20 μg *Tribolium castaneum* PINK1 (expressed in *E. coli*; Ubiquigent: 66-0043-050) or 10 μg human GRK2 (Invitrogen: PV3361) were combined in kinase buffer (20 mM Hepes pH 7.4, 10 mM DTT, 0.1 mM EGTA, 0.1 mM ATP and 10 mM MgCl2) and the reactions allowed to proceed at 37°C for 4 hours or overnight.

Mass spectrometric analysis of Mfn2 phosphopeptides

Preparation of peptides for nano-LC-MS. The in vitro kinase solution that contained 10 μg of Mfn2 was spiked (10 μL) with a mixture of five carrier proteins (10 μg each). The mixture consisted of human apo-transferrin (Sigma, T4382), bovine α-casein (Sigma, C6780), bovine β-casein (Sigma, C6905), bovine ribonuclease (Sigma, R7884), and bovine albumin (Sigma A7030) in 100 mM Tris buffer, pH 7.6 with 4% SDS and 100 mM DTT. The sample was lyophilized overnight in a VirTis AdVantage Lyophilizer (SP Scientific).
Peptides were prepared using a modified filter-aided sample preparation method: dried sample was dissolved in 60 μL of Tris buffer, pH 7.6 that contained 4% SDS and 100 mM DTT and denatured by heating (95ºC) for 5 min. The sample was then alkylated with 50 mM iodoacetamide (Sigma, A3221) for 1 h at room temperature in the dark. After the addition of 1 ml of 50 mM ammonium bicarbonate buffer (pH 8.5) containing 8M urea (UA) and vortexing, equal volumes of the samples were transferred to two YM-30 filter units (Millipore, Ref No. MRCF0R030) and spun for 14 min at 10,000 rcf (Eppendorf, Model No. 5424). Filters were washed with 200 μl of UA and the spin-wash cycle was repeated twice. The sample was then exchanged into digest buffer with the addition of 200 μl of ammonium bicarbonate buffer, pH 8.5 (ABC) and centrifugation (11,000 rcf) for 10 min. After transferring the upper filter unit to a new collection tube, 80 μL of the ABC buffer was added and the sample was digested with trypsin (1 μg) for 4h at 37ºC. The digestion was continued overnight after another addition of trypsin. Filter units were then spun at 11,000 rcf for 10 min with a subsequent filter washing step with 0.5 M NaCl (50 μL) followed by centrifugation (14,000 rcf for 10 min). The digest was then extracted three times with 1 ml of ethyl acetate and acidified with trifluoroacetic acid (TFA) (50%) to a final concentration of 1%. The pH was < 2.0 using pH paper. Solid phase extraction of the peptides was performed using sequential, robotic pipetting with C4 and porous graphite carbon micro-tips (Glygen). The peptides were eluted with 60% acetonitrile in 0.1% TFA and pooled for drying in a Speed-Vac (Thermo Scientific, Model No. Savant DNA 120 concentrator)

after adding TFA to 5%. The peptides were dissolved in 20 µL of 1% acetonitrile in water. An aliquot (10%) was removed for quantification using the Pierce Quantitative Fluorometric Peptide Assay kit (Thermo Scientific, Cat. No. 23290). The remaining sample was transferred to an autosampler vial (Sun-Sri, Cat. No. 200046), dried in the SpeedVac and dissolved in 2.7 µL of 0.1%TFA.

Nano-LC-MS/MS Analysis of Phosphopeptides — The samples were loaded (2.5 µL) at a constant pressure of 700 bar at 100% of mobile phase solvent A (0.1%FA) onto a 75 µm i.d. × 50 cm Acclaim® PepMap 100 C18 RSLC column (Thermo-Fisher Scientific) using an EASY nanoLC (Thermo Fisher Scientific). Before sample loading the column was equilibrated with 100% A using 20µL at 700 bar. Peptide chromatography was initiated with A containing 2% B (100% ACN, 0.1%FA) for 5 min, then linear increased to 20% B over 100 min, to 32% B over 20 min, to 95% B over 1 min and held at 95% B for 7 min, at a flow rate of 300 nL/min. The data dependent mode analysis was performed with in the Orbitrap mass analyzer (Thermo-Fisher Scientific Q-Exactive™ Plus Hybrid Quadrupole-Orbitrap™ mass spectrometer) with a scan range of *m/z* = 375 to 1500 and a mass resolving power set to 70,000. Ten data-dependent high-energy collisional dissociations were performed with a mass resolving power set to 17,500, a fixed lower value of *m/z* = 100, an isolation width of 2 Da, and a normalized collision energy of 27. The maximum injection time was 60 ms for parent-ion accumulations and 60 ms for product-ion analysis. The parent ions that were selected for MS2 were dynamically excluded for 20 sec. The automatic gain control was set at a target ion value of 1e6 for MS1 scans and 1e5 for MS2 acquisition. Peptide ions with charge states of one or > 8 were excluded for CID acquisition.

Phosphopeptide data from the PINK kinase reactions were also acquired in targeted mode. The full-scan mass spectra were acquired by the Orbitrap mass analyzer with a scan range of *m/z* = 350 – 2000 and a mass resolving power set to 70,000. The CID spectra were acquired at resolving power of 17,500 with maximum injection time of 120 ms. The loop count was set to 4 and the isolation width was 2 Da. The acquisition of CID spectra were triggered by an inclusion list of four *m/z* values for the +2 and +3 charge state of the natural abundance phosphorylated and non-phosphorylated peptide (see Supplemental Table S1 for values). An AGC target value of 3e6 was used for MS scans and 2e5 for MS/MS scans. The unprocessed LC-MS data were analyzed using SKYLINE (version 3.6.9).

The high-resolution ion chromatograms for the **y** ion series from the CID phosphopeptide spectra shown in Figure 1G were acquired during the LC-MS analysis of the tryptic digest of human recombinant Mfn2 after phosphorylation with PINK1. The corresponding chromatograms from the synthetic, isotope-labeled phosphopeptide co-eluted with the PINK1 product and all ions were observed with the same proportional intensities in the CID spectra as shown in the adjacent stacked bar charts, confirming the sequence identity and phosphorylated residue location. The expected mass increment of 10 Da from the Arg-[$^{13}C_6$] [$^{15}N_4$] residue was observed for all **y** ions in the CID spectra of the synthetic phosphopeptide. The spectra from the PINK1 phosphopeptide product and the synthetic phosphopeptide were acquired from the triply charged parent ions at *m/z* = 446.543 and *m/z* = 449.880, respectively. The site of phosphorylation was confirmed from the series of **y** ions with neutral losses of the phosphate moiety (H_3PO_4) that were observed **as** $\mathbf{y_8}$**-** $\mathbf{H_3PO_4}$ (*m/z* = 882.427*)*, and $\mathbf{y_7}$**-** $\mathbf{H_3PO_4}$ $^{+2}$ (*m/z* = 384.203*)*. The same ion series was observed in the CID spectrum of the synthetic peptide with the expected 10 Da mass increment, $\mathbf{y_8}$**-** $\mathbf{H_3PO_4}$ (*m/z* = 892.432*)* and $\mathbf{y_7}$**-** $\mathbf{H_3PO_4}$ (*m/z*

= 777.404*)*. Using the synthetic phosphorylated and non-phosphorylated peptides, we determined that the phosphopeptide consistently eluted 9.5 – 10.5 min later in all LC-MS analyses. We also analyzed all tandem spectra that were acquired from a precursor ion at *m/z* = 446.543 for any evidence of phosphorylation at Ser-378 in replicate PINK1 experiments, GRK phosphorylation experiments, and in a digest of the recombinant Mfn2 protein without added kinase. Phosphopeptides with the Ser-378 site were only observed from the PINK1 phosphorylation experiments.

Dextran uptake assays of dynamin function

Wild-type MEFs (100,000 cells) were grown on cover slips. When they reached 60% confluency they were washed with serum-free DMEM. Subsequently, cells were incubated in serum-free DMEM containing either 1 μM compound A; B; B/A-L; dynasore (Calbiochem) or DMSO only (vehicle) for 30 min at 37°C. AF594-labelled 10,000 MW Dextran (Invitrogen) was then added to a final concentration of 0.5 mg/ml and incubated for additional 10 min. at 37°C. Internalization was stopped by washing three-times with ice-cold PBS. Residual dextran was removed by washing with 0.1M Na acetate, 0.05M NaCl for 10 min. Samples were fixed in 4% PFA followed by confocal microscopy analysis.

Confocal live cell studies of mitochondria

Confocal imaging used a Nikon Ti Confocal microscope equipped with a 60×1.3NA oil immersion objective. All live cells were grown on cover slips loaded onto a chamber (Warner instrument, RC-40LP) in modified Krebs-Henseleit buffer (138 mM NaCl, 3.7 mM KCl, 1.2 mM KH2PO4, 15 mM Glucose, 20 mM HEPES and 1 mM CaCl2) at room temperature.
Cells were excited with 408 nm (Hoechst), 561 nm (MitoTracker Green and Calcein AM, GFP), or 637 nm (TMRE, MitoTracker Orange, Ethidium homodimer-1, and AF594- Dextran) laser diodes. For mitochondrial elongation studies mitochondrial aspect ratio (long axis/short axis) was calculated using automated edge detection and Image J software. Mitochondrial depolarization was calculated as % of green mitochondria visualized on MitoTracker Green and TMRE merged images, expressed as green/(green + yellow mitochondria) × 100.

Identification and *de novo* design of small molecule mitofusin agonists

We generated a pharmacophore model based on the interactions of HR1 and HR2 domains in the calculated structural model of Mfn2 in the closed conformation (3). The key features included hydrophobic interactions involving Mfn2 HR1: Val372 and Met376, and aromatic interactions and hydrogen bonding involving Mfn2 HR1 His380. Although our pharmacophore model did not structurally model mitofusin agonist minipeptide HR1 (367-384), we note that peptide residues Val6, Met10, and His14 correspond to Mfn2 HR1: Val372, Met376 and His380. A library comprising ~14 million commercially available compounds was prepared *in silico* and evaluated using PHASE to fit these criteria. Top ranked hits were clustered, and filtered based on pharmacological properties using Qikprop. The top 55 commercially available small molecules conforming to the model were selected for functional screening and purchased in 1 mg aliquots. Each compound was dissolved to a stock concentration of 10 mM in DMSO and applied to Mfn2 null MEFs overnight at a final concentration of 1 μM. Eleven of the library members were not soluble in DMSO at the required concentration. The 44 fully soluble compounds were screened in groups of 6 at a time for cytotoxicity (calcein AM/ethidium homodimer staining; ThermoFisher LIVE/DEAD Assay cat #L3224) and fusogenicity (increase in mitochondrial aspect ratio; MitoTracker Orange staining) compared to cells treated overnight with 5 μM of the parent HR1 367-384 mitofusin agonist peptide (positive control) or vehicle (DMSO). Images were acquired by confocal microscopy. Each compound was scored for fusogenicity (**Supplemental Figure S17A**) and % cell death (**Supplemental Figure S17B**). Pharmacophore model fit generally correlated with actual fusogenic activity (Pearson correlation coefficient r=0.214; **Supplemental Figure S17A, *inset*; Supplemental dataset 2**).

Of nine compounds exhibiting apparent fusogenic activity on the initial screen (defined as an increase in mitochondrial aspect ratio to >5 after 24h exposure to 1 μM compound), one (A8) was mildly cytotoxic and therefore did not undergo further evaluation. The remaining eight candidate fusogenic compounds were evaluated in a second series of experiments for their ability to provoke dose-dependent mitochondrial elongation. Fusogenicity of six compounds was confirmed, with EC_{50} values between ~25 nM and 150 nM (**Supplemental Figure S18; Supplemental dataset 2**). Two compounds (D9 and A9) failed validation in the secondary screen.

Our results defining a minimal fusogenic HR1 peptide (see Figure 1B), identifying function-critical amino acids within the minipeptide (see Figure 1C), and defining HR1-HR2 interacting amino acids through binding assays (Figures 1E and 1F) suggested that our previously published Mfn2 HR1-HR2 interaction model was imperfect (3), thus providing a likely reason for the poor correlation between *in silico* pharmacophore model fit of compounds B1 and A10 and their actual fusogenicity: Val372 was proven to be functionally dispensable and His380 paired with Asp725 rather than Lys720 as indicated in the original model (3). Moreover, our studies revealed that phosphorylation of Ser378 in both the mitofusin agonist peptide and intact Mfn2 protein can change amino acids presented to the HR1-HR2 interface (see Figure 2A); this key transitional feature was not part of the initial model. Compounds A10 and B1 (which ranked 4th and 2nd in fusogencity, but 27th and 31st in fit to the pharmacophore model) and their chemosimilars conformed well to an Mfn2 HR1-HR2 interaction model incorporating these biological findings, as depicted in Supplemental Figure S1. These two compounds were therefore purified (**Supplemental Figure S19**) and used in subsequent studies.

Our ultimate goal was to design mitofusin agonists having optimal activity profiles. (Here, a "fusogenic compound" is defined as promoting mitochondrial elongation without a clearly defined mechanism, while a "mitofusin agonist" is a fusogenic compound that binds to the Mfn2 HR2 minipeptide target domain, promotes Mfn2 opening, and loses its fusogenic activity when endogenous mitofusin proteins are not present). Molecular modeling of class A and B agonists assumed that the minipeptide α-helix is comprised of 3.6 amino acids per turn with a 1.4 A pitch advance per amino acid, resulting in a distance of ~5.4 A between amino acids of adjacent turns. Aliphatic backbones assumed a distance between single bonded carbons of 1.54 A. Structures were created or edited using Marvin JS at the MolPort website (https://www.molport.com/shop/index) and available chemical analogs (chemosimilars; **Supplemental dataset 3**) identified using the search function and a similarity parameter of 0.5.

Chemical synthesis, purification and analyses of novel small molecule mitofusin agonists

Four A-B chimeric molecules designed to incorporate different characteristics of Cpds A and B (**Supplemental dataset 4**) were synthesized de novo:

Chimera B-A/l – (1-(2-((5-cyclopropyl-4-phenyl-4H-1,2,4-triazol-3-yl)thio)ethyl)-3-(2-methylcyclohexyl)urea) was synthesized by Enamine Ltd as a racemic mixture (**fig. S20**). **Step A:** 5-Cyclopropyl-4-phenyl-4H-1,2,4-triazole-3-thiol (**1)** (1 mmol) was dissolved in 1 mL of CH_3OH/H_2O (50:50), then NaOH (1 mmol) was added, stirred for 10 min, and 2-(boc-amino)ethyl bromide (**2)** (1 mmol) was added at 25 ºC. The reaction was allowed to stir for 3 hours then poured into 10 mL water. The precipitate was filtered and dried to get a solid. The crude product was dissolved in 10 ml of trifluoroacetic acid (TFA), and heated at 50 ºC for 10 h to remove the solvent and 10ml of water and NaOH (1 mmol) were added. The mixture was stirred at room temperature for 1 h, filtered, and washed with water (50 ml). The residue was purified using reversed phase high-performance liquid chromatography RP-HPLC. Yield: 52 %. **Step B:** 2-((5-Cyclopropyl-4-phenyl-4H-1,2,4-triazol-3-yl)thio)ethan-1-amine (**3**) (0.5 mmol) and 1,1′-carbonyldiimidazole (CDI) (1 mmol) were dissolved in 0.6 ml CH_3CN, the mixture was kept at a temperature of 70 ºC for 1 h, and then the 2-methyl-cyclohexylamine (**4**) (0.5 mmol) was added. The mixture was heated for 2 hours at 70 ºC, then filtered, and evaporated. The residue was purified using RP-HPLC to give the desired product as a white solid; Purity: 99.99% (**fig. S21A**); Yield: 32 %; C21H29N5OS; MW 399.5. Liquid chromatography with high-resolution mass spectrometry using electrospray ionization LC-HRMS (ESI) with expected m/z 399.25 showed exact mass found 400.2 $[M + H]^+$ (**fig. S21B**). Chemical structure was confirmed by proton nuclear magnetic resonance (^1H NMR) and carbon-13 nuclear magnetic resonance (^{13}C NMR) (**fig. S22**). ^1H NMR (400 MHz, DMSO-*d*6) δ 7.60 (m, 3H), 7.48 (m, 2H), 5.95 (dt, 1H), 5.81 (dd, 1H), 3.26 (q, 2H), 3.07 (t, 2H), 3.00 (m, 1H), 1.62 (m, 4H), 0.99 (m, 10H), 0.81 (d, 2H), 0.75* (d, 1H). ^{13}C NMR (126 MHz, $CDCl_3$) δ 157.45, 156.97, 149.14, 133.14, 129.74, 127.34, 53.83, 48.83, 39.00, 34.12, 33.92, 32.69, 25.39, 25.30, 19.20, 7.15, 5.67.

Chimera B-A/s (2-((5-cyclopropyl-4-phenyl-4H-1,2,4-triazol-3-yl)thio)-N-(2-methylcyclohexyl)propanamide) was synthesized by Enamine as a racemic mixture (**fig. S23**): 5-Cyclopropyl-4-phenyl-4H-1,2,4-triazole-3-thiol (**1)** (0.5 mmol) was dissolved in 1 mL of CH_3OH, then KOH (0.5 mmol) was added, stirred for 10 min, and then 2-chloro-N-(2-methylcyclohexyl)propanamide (**2)** (0.5 mmol), was added at room temperature. The reaction was allowed to stir for 3 hours then poured into 10 mL water. The precipitate was filtered and dried, then was purified using RP-HPLC to give the title compound as a light brown solid; Purity: 99.99% (**fig. S24A**); Yield: 43 %; C21H28N4OS; MW 384.54. LC-HRMS (ESI): expected m/z 384.24, exact mass found 385.2 $[M + H]^+$ (**fig. S24B**). Chemical structure was confirmed by ^1H NMR and ^{13}C NMR (**fig. S25**): ^1H NMR (500 MHz, DMSO-d_6) δ 8.01 (dd, 1H), 7.60 (m, 3H), 7.45 (m, 2H), 4.27 (qd, 1H), 3.14 (qd, 1H), 1.65 (m, 3H), 1.57 (m, 2H), 1.44 (d, 2H), 1.40 (d, 1H), 1.16 (m, 4H), 0.93 (m, 3H), 0.86 (m, 2H), 0.78 (d, 2H), 0.71* (d, 1H). ^{13}C NMR (126 MHz, DMSO-d_6) δ 158.01, 139.15, 129.31, 128.75, 127.18, 54.27, 49.26, 39.36, 38.56, 35.24, 34.61, 34.48, 31.88, 31.83, 25.88, 25.79, 19.70.

Chimera A-B/l: (2-(3-(2-(benzylthio)ethyl)ureido)-5,6-dihydro-4H-cyclopenta[b]thiophene-3-carboxamide) was synthesized by Enamine Ltd (**fig. S26**). **Step A**: Under an argon atmosphere, into a reaction vessel of 2-amino-5,6-dihydro-4H-cyclopenta[b]thiophene-3-carboxamide (**1**) (1.0 mmol), potassium iodide (0.8 mmol), potassium carbonate (1.0 mmol), N,N-dimethylformamide (DMF) 1 mL and 2,2,2-trifluoroethyl chloroformate (**2)** (1.0 mmol) were added. The reaction vessel was heated to 80 °C, and the mixture was stirred for 12 hours. The reaction vessel was cooled to room temperature, and ethyl acetate 100 mL was added. The organic layer was washed with water (50 mL), saturated brine (50 mL), and dried over sodium sulfate. The sodium sulfate and the solvent were distilled off. Compound 3 was purified using RP-HPLC. Yield: 54%. **Step B**: To a solution of 2 mmol of a 2,2,2-trifluoroethyl (3-carbamoyl-5,6-dihydro-4H-cyclopenta[b]thiophen-2-yl)carbamate (**3)** and 2 mmol of an 2-(benzylthio)ethan-1-amine (**4)** in 2 mL of acetonitrile, 0.2 mmol of 1,8-diazabicyclo[5.4.0]undec-7-ene (DBU) was added. The reaction mixture was heated at 80 °C for 4 h. Then 0.5-2 mL of water was added to the hot reaction mixture. The product precipitated from the solution upon cooling to room temperature then filtered and concentrated in vacuum. The residue was purified using RP-HPLC to give the title compound as a brown solid. Purity: 97.56% (**fig. S27A**); Yield: 51%; C18H21N3O2S2; MW 375.51; LC-HRMS (ESI): expected m/z 375.13, exact mass found 376.0 $[M + H]^+$ (**fig. S27B**); Structure was confirmed by ^{1}H NMR and ^{13}C NMR (**fig. S28**): ^{1}H NMR (400 MHz, DMSO-d_6) δ 10.87 (s, 1H), 7.88 (s, 1H), 7.31 (m, 6H), 6.47 (s, 1H), 3.76 (s, 2H), 3.25 (q, 2H), 2.86 (t, 2H), 2.73 (t, 2H), 2.48 (m, 2H), 2.31 (p, 2H). ^{13}C NMR (126 MHz, DMSO-d_6) δ 167.20, 153.47, 151.94, 138.52, 128.88, 128.84, 128.32, 107.82, 34.74, 30.66, 29.30, 28.22, 27.52.

Chimera A-B/s: (2-(2-(benzylthio)propanamido)-5,6-dihydro-4H-cyclopenta[b]thiophene-3-carboxamide) was synthesized by Enamine Ltd as a racemic mixture (**fig. S29**): Phenylmethanethiol (**1**) (0.5 mmol) was dissolved in 1 mL of CH_3OH , then ethylbis(propan-2-yl)amine (0.55 mmol) was added, stirred for 10 min, and then 2-(2-chloropropanamido)-4H,5H,6H-cyclopenta[b]thiophene-3-carboxamide (**2)** (0.5 mmol) was added. The reaction was allowed to stir at room temperature for 3 hours, and then poured into 10 mL water. The precipitate was filtered and dried, then was purified using RP-HPLC to give the title compound as a yellow solid; Purity: 98.76% (**fig. S30A**); Yield: 37 %; C18H20N2O2S2; MW 360.49; LC-HRMS (ESI): expected m/z 360.12, exact mass found 361.2 [M + H]+ (**fig. S30B**); Structure was confirmed by1H NMR and 13C NMR (**fig. S31**): ^{1}H NMR (500 MHz, DMSO-d_6) δ 12.49 (s, 1H), 7.64 (s, 1H), 7.33 (d, 2H), 7.28 (t, 2H), 7.22 (t, 1H), 6.70 (s, 1H), 3.83 (AB-system, 2H), 3.63 (q, 1H), 2.92 (t, 2H), 2.79 (t, 2H), 2.36 (q, 2H), 1.40 (d, 3H). ^{13}C NMR (126 MHz, DMSO-d_6) δ 168.77, 167.06, 148.07, 139.07, 137.35, 131.71, 128.91, 128.37, 126.99, 111.30, 42.52, 34.88, 29.03, 28.22, 27.68, 17.57.

Purification methods

Preparative HPLC

Purification was performed using HPLC (H_2O – MeOH; Agilent 1260 Infinity systems equipped with DAD and mass-detectors. Waters Sunfire C18 OBD Prep Column, 100Å, 5 µm, 19 mm X 100 mm with SunFire C18 Prep Guard Cartridge, 100Å, 10 µm, 19 mm X 10 mm) The material was dissolved in 0.7 mL DMSO. Flow: 30mL/min. Purity of the obtained fractions was checked via the analytical LCMS. Spectra were recorded for each fraction as it was obtained straight after chromatography in the solution form. The solvent was evaporated in the flow of N_2 at 80°C. On the basis of post-chromatography LCMS analysis fractions were united. Solid fractions were dissolved in 0.5 mL MeOH and transferred into pre-weighted marked vials. Obtained solutions were again evaporated in the flow of N_2 at 80°C. After drying, products were finally characterized by LCMS and ^{1}H NMR and ^{13}C NMR.

Analytical methods

HPLC/HRMS (ESI)

LC/MS analysis was carried out using Agilent 1100 Series LC/MSD system with DAD\ELSD and Agilent LC\MSD VL (G1956A), SL (G1956B) mass-spectrometer or Agilent 1200 Series LC/MSD system with DAD\ELSD and Agilent LC\MSD SL (G6130A), SL (G6140A) mass-spectrometer. All the LC/MS data were obtained using positive/negative mode switching. The compounds were separated using a Zorbax SB-C18 1.8 μm 4.6x15mm Rapid Resolution cartridge (PN 821975-932) under a mobile phase (A – acetonitrile, 0.1% formic acid; B – water (0.1% formic acid)). Flow rate: 3ml/min; Gradient 0 min – 100% B; 0.01 min – 100% B; 1.5 min - 0% B; 1.8 min - 0% B; 1.81 min - 100% B; Injection volume 1μl; Ionization mode atmospheric pressure chemical ionization (APCI); Scan range m/z 80-1000.

NMR

^{1}H and ^{13}C NMR spectra were recorded at ambient temperature using Bruker AVANCE DRX 500; Varian UNITYplus 400 spectrometers.

Mouse hippocampal neuron preparation, culture, and live cell imaging

Neonatal mouse hippocampal neurons were cultured from brains of one day old Mfn2 T105M or non-transgenic sibling mouse pups as described (*28*). After 10 days of differentiating culture neurons were infected with Adeno-Cre to induce Mfn2 T105M expression or Adeno-βgal as a control (50 MOI). After an additional 72 hours mitofusin agonists or DMSO vehicle were added. For static confocal imaging neuronal mitochondria were labeled with adenoviral-expressed mitoGFP plus TMRE. Autophagy was measured by LC3 aggregation in neurons infected with adenoviral LC3-GFP. For time-lapse studies of mitochondrial trafficking bi-cistronic Adeno-Cre/GFP marked Cre expression and mitochondria were labeled with adeno-mitoDsRed. Confocal live cell images were acquired with a time-lapse of 1 frame every 90 seconds for 1 hour.

HB9-Cre/Mfn2 T105M mouse creation and sciatic nerve studies

All mouse procedures were approved by the Institutional Animal Care and Use Committee of Washington University in St. Louis. C57BL/6-Gt(ROSA)26Sortm1(CAG-MFN2*T105M)Dple/J (stock no. 025322 donated by David Pleasure, University of California Davis) (*29*) and B6.129S1-Mnx1tm4(cre)Tmj/J (here referred to as HB9-Cre; stock no. 006600 donated by Thomas Jessel of Columbia University) (*30*) were purchased from The Jackson Laboratory. The HB9-Cre driver was bred onto the ROSA26 flox-stop Mfn2 T105 transgene to induce Mfn2 T105M expression in motor neurons. Age- and sex-matched C57/b6 mice or mice carrying the Mfn2 T105 flox-stop transgene in the absence of Cre were studied as normal controls.

Sciatic nerves of 12-18 week old male or female Mfn2 T105M mice were removed en bloc with the lumbar spine and axotomy at the tibial nerve, stained with TMEM (200 μM) for 30 minutes in prewarmed Neurobasal Medium without phenol red (Thermo Fisher Scientific) at room temperature, washed, and maintained on the stage of a Nikon A1Rsi Confocal Microscope at 37degrees C for time-lapse confocal studies. Images were acquired with a 40x oil immersion objective at 1 frame every 5 or 10 seconds for sequential 10 minute periods. Mitofusin agonist chimera B-A/l was added after the first 10 minute imaging period (final concentrations of 1 or 5 μM) and nerve axons imaged for another 40 minutes. Because there was no difference in mitochondrial trafficking or response to mitofusin agonist between male and female mice, the data were combined.

Statistical methods
All data are reported as mean±SEM. Statistical comparisons (two-sided) used one-way ANOVA and Tukey's tests for multiple groups or Student's t-test for paired comparisons. $p<0.05$ was considered significant.

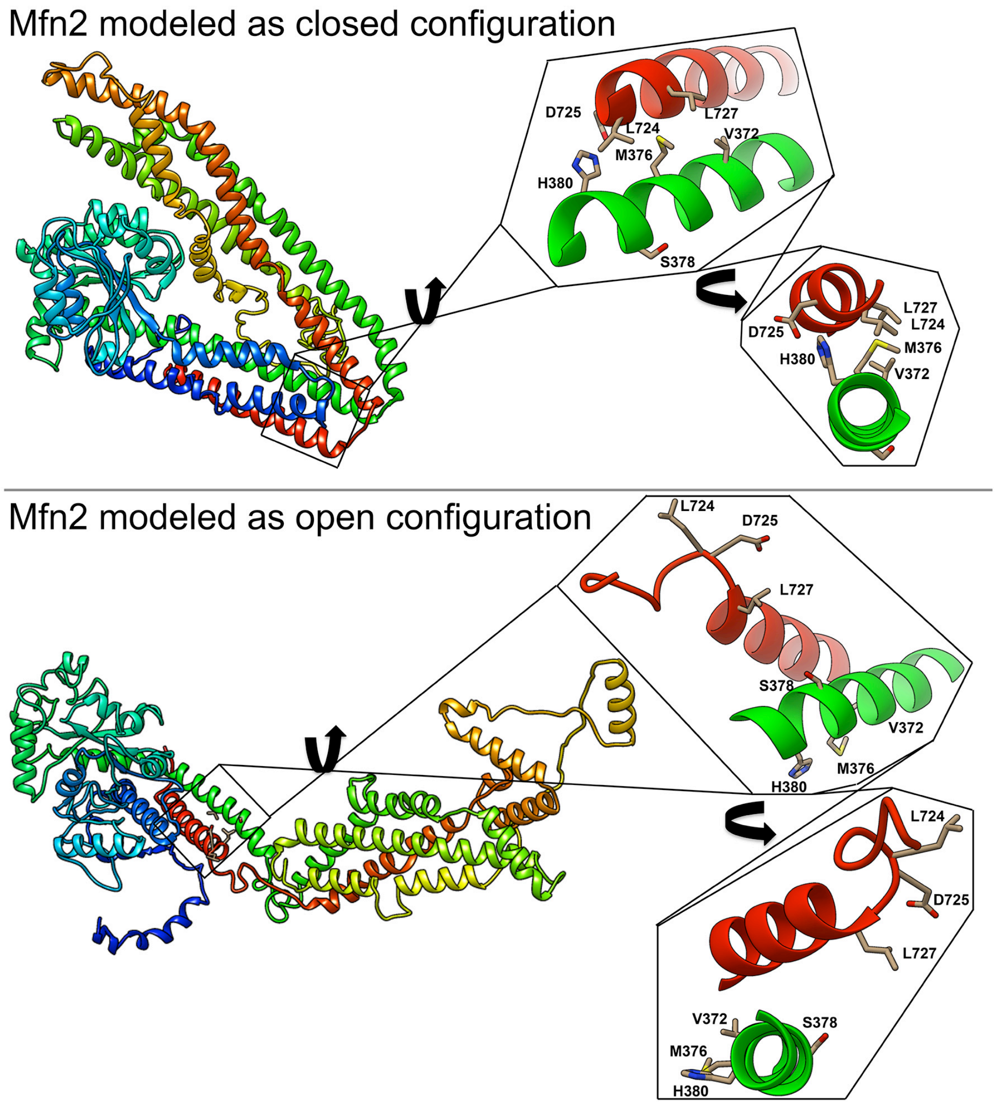

Fig. S1. *Hypothetical structures of human Mfn2.* **(top)** Mfn2 computationally modeled in a closed configuration based on structural homology with *Homo sapiens* Mfn1 and *Arabidopsis thaliana* dynamin-related protein (BDRP). **(bottom)** Mfn2 computationally modeled in an open configuration based on structural homology with *Homo sapiens* Opa1. The first heptad repeat (HR1) domain is green and the carboxyl-terminal second heptad repeat (HR2) domain is red. Exploded areas show critical predicted HR1-HR2 interactions for the two conformations in orthogonal views.

```
                          10        20        30        40        50        60        70
                  ....|....|....|....|....|....|....|....|....|....|....|....|....|....|....|....
Human             MSLLFSRCN-SIVTVKKNKRHMAEVNASPLKHFVTAKKKINGIFEQLGAYIQESATFLEDTYRNAELDPVTTEEQVLDVK
Chimpanzee        MSLLFSRCN-SIVTVKKDKRHMAEVNASPLKHFVTAKKKINGIFEQLGAYIQESATFLEDTYRNAELDPVTTEEQVLDVK
Gorilla           MSLLFSRCN-SIVTVKKDKRHMAEVNASPLKHFVTAKKKINGIFEQLGAYIQESATFLEDTYRNAELDPVTTEEQVLDVK
Monkey            MSLLFSRCN-TIVTVKKDKRHMAEVNASPLKHFVTAKKKINGIFEQLGAYIQESATFLEDTYRNAELDPVTTEEQVLDVK
Macaque           MSLLFSRCN-TIVTVKKDKRHMAEVNASPLKHFVTAKKKINGIFEQLGAYIQESATFLEDTYRNAELDPVTTEEQVLDVK
Marmoset          MSLLFSRCN-SIVTVKKDKRHMAEVNASPLKHFVTAKKKINGIFEQLGAYIQESATFLEDTYRNAELDPVTTEEQVLDVK
Bushbaby          MSLLFSRCN-SIVTVKKDKRHMAEVNASPLKHFVTAKKKINGIFEQLGAYIQESATFLEDTYRNAELDPVTTEEQVLDVK
Lemur             MSLLFSRCN-SIATVKKDKRHMAEVNASPLKHFVTAKKKINGIFEQLGAYIQESATFLEDTYRNAELDPVTTEEQVLDVK
Gibbon            MSLLFSRCN-SIVTVKKDKRHMAEVNASPLKHFVTAKKKINGIFEQLGAYIQESATFLEDTYRNAELDPVTTEEQVLDVK
Elephant          MSLLFSRCN-SIVTVKKDKRHMAEVNASPLKHFVTAKKKINGIFEQLGAYIQESATFLEDTYRNAELDPVTTEEQFLDVK
Armadillo         MSLLFSRCN-SIVTVKKDKRHMAEVNASPLKHFVTAKKKINGIFEQLGAYIQESATFLEDTHRNAELDPVTTEEQVLDVK
Cat               MSLLFSRCN-SIVTVKKDKRHMAEVNASPLKHFVTAKKKINGIFEQLGAYIQESATFLEDTYRNAELDPVTTEEQVVDVK
Dog               MSLLFPRCN-SIVTVKKDKRHMAEVNASPLKHFVTAKKKINGIFEQLGAYIQESATFLEDTYRNAELDPVTTEEQVLDVK
Ferret            MSLLFSRCN-SIVTVKKDKRHMAEVNASPLKHFVTAKKKINGIFEQLGAYIQESATFLEDTHRNAELDPVTTEEQVLDVK
Boar              MSLLFSRCN-SIVTVKKDKRHMAEVNASPLKHFVTAKKKINGIFEQLGAYIQESATFLEDTYRNEELDPVTTEEQVLDVK
Dolphin           MSLLFSRCN-SIITVKKDKRHMAEVNASPLKHFVTAKKKINGIFEQLGAYIQESATFLEDTYRNAELDPVTTEEQVLDVR
Sheep             MSLLFSRCN-SIVTVKKDKRHMAEVNASPLKHFVTAKKKINGIFEQLGAYIQESATFLEETYRNAELDPVTTEEQVLDVK
Squirrel          MSLLFSRCN-SIVAVKKDKRHMAEVNASPLKHFVTAKKKINGIFEQLGAYIQESATFLEDTYRNAELDPVTTEEQVLDVK
Guinea pig        MSLLFSRCN-PIVTVKKDKRHMAEVNASPLKHFVTAKKKINGIFEQLGAYIQESAAFLEDTYRNAELDPVTTEEQVLDVK
Rat               MSLLFSRCN-SIVTVKKDKRHMAEVNASPLKHFVTAKKKINGIFEQLGAYIQESAGFLEDTHRNTELDPVTTEEQVLDVK
Mouse             MSLLFSRCN-SIVTVKKDKRHMAEVNASPLKHFVTAKKKINGIFEQLGAYIQESASFLEDTHRNTELDPVTTEEQVLDVK
Horse             MSVLFPRCN-SIVTVKKDKRHMAEVNASPLKHFVTAKKKINGIFEQLGAYIQESATFLEDTYRNAELDPVTTEEQVLDVK
Opossum           MSLIFSHSN-SIVSIKKDKRHMAEVNASPLKHFVTAKKKINGIFEQLGAYIQESATFLEDTHRNVELDPVTTEEQVLEVK
Collrd flyctchr   MSLLFTRSN-SIVAVKKDKRHMAEVNASPLKHFVTAKKKINGIFEQLAAYINESSSFLEETHKNAELDPVTTEEQVLEVK
Zebra finch       MSLLFTRSN-SIVAVKKDKRHMAEVNASPLKHFVTAKKKINGIFEQLAAYINESSLFLEETHKNAELDPVTTEEQVLEVK
Chicken           MSLLFTRSK-SIVAVKKDKRHMAEVNASPLKHFVTAKKKINGIFEQLAAYINESSSFLEETHKNVELDPVTTEEQVLEVK
Turkey            MSLLFTRSK-SIVAVKKDKRHMAEVNASPLKHFVTAKKKINGIFEQLAAYINESSSFLEETHKNVELDPVTTEEQVLEVK
Turtle            MSLLFTCSK-SIVAVKKDKRHMAEVNASPLKHFVTAKKKINGIFEQLAAYIQESATFLEETHRNVELDPVTTEEQVLEVK
Pufferfish        MSLVFSRHNTNAVHGKKDKRLMAEVNASPLKHFVTAKKKINGIFEQLGAYIKESASFLEDTYRNEELDPVTTEEQVQEVC
Tilapia           MSLVFPRLSTKTFHSKKEKRIMAEVNASPLKHFVTAKKKINGIFEQLGAYIKESASFLEDAYKSEELDPVATEEQVQEVE
Stickleback       MSLVFPRPNTNAVHGKKDKRLMAEVNASPLKHFVTAKKKINGIFEQLGVYIKESASFLDDTHKNEELDPVTTEEQVQEVR
Cod               MSLVFPRPNSNSIHGKKDKRLMAEVNASPLKHFVTAKKKINGIFEQLGAYIKESSSFLEETYKSDELDPVTTEEQVQEVR
Platyfish         MSISVPRPSPLKFQCKKKNRTMAEVNVSPLKHFVTAKKKINGIFEQLGTYIKESAAFLEDTYKNEQLDPLTTEEQVQEVC
Amazon molly      MSISVSRPNPVQFQCKKKNRTMAEVNVSPLKHFVTAKKKINGIFEQLATYIKESAAFLEDTYKNEQLDPLTTEEQVQEVC
Spotted gar       MSLIFSRTN--TAISKKDKRLMAEVNASPLKHFVTAKKKINGIFEQLGAYIKESSAFLEETYKNEDLDPIATEEQVMEVK
Cave fish         MSLVFPRPN-TSAIGKKDKRLMAEVNASPLKHFVTAKKKINGIFEQLGAYIKESSAFLEETYSNEELDPVTTEEQVAEVR
Zebrafish         MSLVFPRPN-TSVIGKKDKRLMAEVNASPLKHFVTAKKKINGIFEQLGAYIKESSAFLEETYSNEELDPVTTEEQVAEVR
Coelacanth        MSLLFSRSN-SVATGKKDKRLMAEVNASPLKHFVTAKKKINGIFEQLAVYIKESSAFLEETHKNDELDPITTEEQVSEVK
Frog              MSLLFSRPI-IKVTTKKDKRFMAEVTASPLKHFVTAKKKINGIFDQLAAYTQESYNFLEETYKDAELDPVASEEQVFEVK
```

```
                  80        90        100       110       120       130       140       150
                  |....|....|....|....|....|....|....|....|....|....|....|....|....|....|....|....
Human             GYLSKVRGISEVLARRHMKVAFFGRTSNGKSTVINAMLWDKVLPSGIGHTTNCFLRVEGTDGHEAFLLTEGSEEKRSAKT
Chimpanzee        GYLSKVRGISEVLARRHMKVAFFGRTSNGKSTVINAMLWDKVLPSGIGHTTNCFLRVEGTDGHEAFLLTEGSEEKRSAKT
Gorilla           GYLSKVRGISEVLARRHMKVAFFGRTSNGKSTVINAMLWDKVLPSGIGHTTNCFLRVEGTDGHEAFLLTEGSEEKRSAKT
Monkey            GYLSKVRGISEVLARRHMKVAFFGRTSNGKSTVINAMLWDKVLPSGIGHTTNCFLRVEGTDGHEAFLLTEGSEEKRSAKT
Macaque           GYLSKVRGISEVLARRHMKVAFFGRTSNGKSTVINAMLWDKVLPSGIGHTTNCFLRVEGTDGHEAFLLTEGSEEKRSAKT
Marmoset          GYLSKVRGISEVLARRHMKVAFFGRTSNGKSTVINAMLWDKVLPSGIGHTTNCFLRVEGTDGHEAFLLTEGSEEKRSAKT
Bushbaby          GYLSKVRGISEVLARRHMKVAFFGRTSNGKSTVINAMLWDKVLPSGIGHTTNCFLRVEGTDGHEAFLLTEGSEEKRSVKT
Lemur             GYLSKVRGISEVLARRHMKVAFFGRTSNGKSTVINAMLWDKVLPSGIGHTTNCFLRVEGTDGHEAFLLTEGSEEKRSVKT
Gibbon            GYLSKVRGISEVLARRHMKVAFFGRTSNGKSTVINAMLWDKVLPSGIGHTTNCFLRVEGTDGHEAFLLTEGSEEKRSAKT
Elephant          GYLSKVRGISEVLARRHMKVAFFGRTSNGKSTVINAMLWDKVLPSGIGHTTNCFLRVEGTDGHEAFLLTEGSEEKKSVKT
Armadillo         GYLSKVRGIGEVLARRHMKVAFFGRTSNGKSTVINAMLWDKVLPSGIGHTTNCFLRVGGTDGHEAFLLTEGSEEKRSVKT
Cat               GYLSKVRGISEVLARRHMKVAFFGRTSNGKSTVINAMLWDKVLPSGIGHTTNCFLRVEGTDGHEAFLLTEGSEEKRSVKT
Dog               GYLSKVRGISEVLARRHMKVAFFGRTSNGKSTVINAMLWDKVLPSGIGHTTNCFLRVEGTDGHEAFLLTEGSEEKRSVKT
Ferret            GYLSKVRGISEVLARRHMKVAFFGRTSNGKSTVINAMLWDKVLPSGIGHTTNCFLRVEGTDGHEAFLLTEGSEEKRSVKT
Boar              GYLSKVRGISEVLARRHMKVAFFGRTSNGKSTVINAMLWDKVLPSGIGHTTNCFLRVEGTDGHEAFLLTEGSEEKRSVKT
Dolphin           GYLSKVRGISEVLARRHMKVAFFGRTSNGKSTVINAMLWDKVLPSGIGHTTNCFLRVEGTDGHEAFLLTEGSEEKRSVKT
Sheep             GYLSKVRGISEVLARRHMKVAFFGRTSNGKSTVINAMLWDKVLPSGIGHTTNCFLRVEGTDGHEAFLLTEGSEEKRSVKT
Squirrel          GYLSKVRGISEVLARRHMKVAFFGRTSNGKSTVINAMLWDKVLPSGIGHTTNCFLRVEGTDGHEAFLLTEGSEEKRSVKT
Guinea pig        GYLSKVRGISEVLARRHMKVAFFGRTSNGKSTVINAMLWDKVLPSGIGHTTNCFLRVGGTEGHEAFLLTEGSEEKRSVKT
Rat               GYLSKVRGISEVLARRHMKVAFFGRTSNGKSTVINAMLWDKVLPSGIGHTTNCFLRVGGTDGHEAFLLTEGSEEKKSVKT
Mouse             GYLSKVRGISEVLARRHMKVAFFGRTSNGKSTVINAMLWDKVLPSGIGHTTNCFLRVGGTDGHEAFLLTEGSEEKKSVKT
Horse             GYLSKVRGISEVLARRHMKVAFFGRTSNGKSTVINAMLWDKVLPSGIGHTTNCFLRVEGTDGHEAFLLTEGSEEKKSVKT
Opossum           AYLAKVKGIGEVLARRHMKVAFFGRTSNGKSTVINAMLWDKVLPSGIGHTTNCFLRVEGTDGHEAFLLTEGSEEKKSVKT
Collrd flyctchr   SYLSKVSGISEVLARRHMKVAFFGRTSNGKSTVINAMLWDKVLPSGIGHTTNCFLRVEGTDGHEAFLLTEGSEEKKSVKT
Zebra finch       GYLSKVSGISEVLARRHMKVAFFGRTSNGKSTVINAMLWDKVLPSGIGHTTNCFLRVEGTDGHEAFLLTEGSEEKKSVKT
Chicken           GYLSKVSGISEVLARRHMKVAFFGRTSNGKSTVINAMLWDKVLPSGIGHTTNCFLRVEGTDGHEAFLLTEGSEEKKSVKT
Turkey            GYLSKVSGISEVLARRHMKVAFFGRTSNGKSTVINAMLWDKVLPSGIGHTTNCFLRVEGTDGHEAFLLTEGSEEKKSVKT
Turtle            GYLSKVSGISEVLARRHMKVAFFGRTSNGKSTVINAMLWDKVLPSGIGHTTNCFLRVEGTEGQDAFLLTEGSEEKRSVKT
Pufferfish        GYLAKVAGIGEVLARRHMKVVFFGRTSNGKSSVINAMLCDKVLPSGIGHTTNCFLRVEGTDGSEAFILTEGSEERKSIKT
Tilapia           GYLAKVTGIGEVLARRHMKVVFFGRTSNGKSSVINAMLCDKVLPSGIGHTTNCFLRVEGTDGNEAFILTGGSEERKNIKT
Stickleback       GYLAKVAGIGEVLARRHMKVVFFGRTSNGKSSVINAMLCDKVLPSGIGHTTNCFLRVEGTDGNEAFLLTEGSEERKSIKT
Cod               GYLAKVAGIGEVLARRHMKVVFFGRTSNGKSSVINAMLCDKVLPSGIGHTTNCFLRVEGTDGNESFLLTEGSEERKSIKT
Platyfish         SYLSKVAGIGEVLARRHMKVVFFGRTSNGKSSVINAMLCDKVLPSGIGHTTNCFLRVEGTDGNDGFLLTEGSEERKSITT
Amazon molly      GYLSKVAGIGEVLARRHMKVVFFGRTSNGKSSVINAMLCDKVLPSGIGHTTNCFLRVEGTDGNEGFLLTEGSEDRKSITT
Spotted gar       GYLSKVAGIGEVLARRHMKVAFFGRTSNGKSSVINAMLWDKVLPSGIGHTTNCFLRVEGTDGNDSYLLTEGSEERKSVNT
Cave fish         GYLSKVAGIGEVLSRRHMKVVFFGRTSNGKSSVINAMLWDKVLPSGIGHTTNCFLRVEGTDGNEAFLLTEGSEERKNVKT
Zebrafish         GYLSKVAGIGEVLSRRHMKVVFFGRTSNGKSSVINAMLWDKVLPSGIGHTTNCFLRVEGTDGNESFLLTEGSDERKSVKT
Coelacanth        SYLSKVAGISEVLARRHMKVAFFGRTSNGKSSVINAMLWDKVLPSGIGHTTNCFLRVEGTEGSEAYLLTEGSEEKRSVKT
Frog              GYLTNVAGISEVLARRHMKVAFFGRTSNGKSSVINAMLWDKVLPSGIGHTTNCFLRVEGTDGNESYLLTGGSEEKRSVKT
```

```
                   160       170       180       190       200         210       220       230
                   |....|....|....|....|....|....|....|....|..  ....|....|....|....|....|....|....|..
Human              VNQLAHALHQDKQLHAGSLVSVMWPNSKCPLLKDDLVLMDS--PGIDVTTELDSWIDKFCLDADVFVLVANSESTLMQTE
Chimpanzee         VNQLAHALHQDKQLHAGSLVSVMWPNSKCPLLKDDLVLMDS--PGIDVTTELDSWIDKFCLDADVFVLVANSESTLMQTE
Gorilla            VNQLAHALHQDKQLHAGSLVSVMWPNSKCPLLKDDLVLMDS--PGIDVTTELDSWIDKFCLDADVFVLVANSESTLMQTE
Monkey             VNQLAHALHQDKQLHAGSLVSVMWPNSKCPLLKDDLVLMDS--PGIDVTTELDSWIDKFCLDADVFVLVANSESTLMQTE
Macaque            VNQLAHALHQDKQLHAGSLVSVMWPNSKCPLLKDDLVLMDS--PGIDVTTELDSWIDKFCLDADVFVLVANSESTLMQTE
Marmoset           VNQLAHALHQDKQLHAGSLVSVMWPNSKCPLLKDDLVLMDS--PGIDVTTELDSWIDKFCLDADVFVLVANSESTLMQTE
Bushbaby           VNQLAHALHQDEQLHAGSLVSVMWPNSKCPLLKDDLVLMDS--PGIDVTTELDSWIDKFCLDADVFVLVANSESTLMQTE
Lemur              VNQLAHALHQDEQLHAGSLVSVMWPNSKCPLLKDDLVLMDS--PGIDVTTELDSWIDKFCLDADVFVLVANSESTLMQTE
Gibbon             VNQLAHALHQDEQLHAGSLVSVMWPNSKCPLLKDDLVLMDS--PGIDVTTELDSWIDKFCLDADVFVLVANSESTLMQTE
Elephant           VNQLAHALHQDEQLHAGSLVSVMWPNSKCPLLKDDLVLMDS--PGIDVTTELDSWIDKFCLDADVFVLVANSESTLMQTE
Armadillo          VNQLAHALHQDEQLHAGSLVSVMWPNSKCSLLKDDLVLMDS--PGIDVTTELDSWIDKFCLDADVFVLVANSESTLMQTE
Cat                VNQLAHALHQDEQLHAGSLVSVMWPNSKCPLLKDDLVLMDS--PGIDVTTELDSWIDKFCLDADVFVLVANSESTLMQTE
Dog                VNQLAHALHQDEQLHAGSLVSVMWPNSKCPLLKDDLVLMDS--PGIDVTTELDSWIDKFCLDADVFVLVANSESTLMQTE
Ferret             VNQLAHALHQDEQLHAGSLVSVMWPNSKCPLLKDDLVLMDS--PGIDVTTELDSWIDKFCLDADVFVLVANSESTLMQTE
Boar               VNQLAHALHQDEQLHAGSLVSVMWPNSKCPLLKDDLVLMDS--PGIDVTTELDSWIDKFCLDADVFVLVANSESTLMQTE
Dolphin            VNQLAHALHQDEQLHAGSLVSVMWPNSKCPLLKDDLVLMDS--PGIDVTTELDSWIDKFCLDADVFVLVANSESTLMQTE
Sheep              VNQLAHALHQDEQLHAGSLVSVMWPNSKCPLLKDDLVLMDS--PGIDVTTELDSWIDKFCLDADVFVLVANSESTLMQTE
Squirrel           VNQLAHALHQDEQLNAGSLVSVMWPNSKCPLLKDDLVLMDS--PGIDVTTELDSWIDKFCLDADVFVLVANSESTLMQTE
Guinea pig         VNQLAHALHQDEQLHAGSLVSVMWPNSKCPLLKDDLVLMDS--PGIDVTTELDSWIDKFCLDADVFVLVANSESTLMQTE
Rat                VNQLAHALHQDEQLHAGSLVSVMWPNSKCPLLKDDLVLMDS--PGIDVTTELDSWIDKFCLDADVFVLVANSESTLMQTE
Mouse              VNQLAHALHQDEQLHAGSMVSVMWPNSKCPLLKDDLVLMDS--PGIDVTTELDSWIDKFCLDADVFVLVANSESTLMQTE
Horse              VNQLAHALHQDEQLHAGSLVSVMWPNSKCPLLKDDLVLMDR--PGLAQPNPPASWVSSRCPEDEHFVLLCGQASPLVQ-E
Opossum            VNQLAHALHQDELLNAGSLVSVMWPNSKCSLLKDDLVLMDS--PGIDVTTELDSWIDKFCLDADVFVLVANSESTLMQTE
Collrd flyctchr    VNQLAHALHQDEHLNAGSLVSVMWPNSKCSLLKDDLVLMDS--PGIDVTTELDSWIDKFCLDADVFVLVANSESTLMQTE
Zebra finch        VNQLAHALHQDEHLNAGSLVSVMWPNSKCSLLKDDLVLMDS--PGIDVTTELDSWIDKFCLDADVFVLVANSESTLMQTE
Chicken            VNQLAHALHQDELLNAGSLVSVMWPNSKCPLLKDDLVLMDS--PGIDVTTELDSWIDKFCLDADVFVLVANSESTLMQTE
Turkey             VNQLAHALHQDELLNAGSLVSVMWPNSKCPLLKDDLVLMDS--PGIDVTTELDSWIDKFCLDADVFVLVANSESTLMQTE
Turtle             VNQLAHALHQNELLNAGSLVSVMWPNSKCPLLKDDLVLMDS--PGIDVTTELDSWIDKFCLDADVFVLVANSESTLMQTE
Pufferfish         VNQLAHALHQDEDLDAGSLVCVMWPKAKCALLRDDLVLVDS--PGIDVTTELDSWIDKFCLDADVFVLVANSESTLMQTE
Tilapia            VNQLAHALHQDEDLDAGSLVCVMWPKAKCALLRDDLVLVDSSSPGIDVTTELDSWIDKFCLDADVFVLVANSESTLMQTE
Stickleback        VNQLAHALHQDEDLDAGSLVCVMWPKAKCALLRDDLVLVDS--PGIDVTTELDSWIDKFCLDADVFVLVANSESTLMQTE
Cod                VNQLAHALHQDELLDAGSLVCVMWPKAKCALLRDDLVLVDS--PGIDVTTELDSWIDKFCLDADVFVLVANSESTLMQTE
Platyfish          VNQLAHALLQDVDLDAGSLVCVMWPKAKCALLRDDLVLLDS--PGIDVTTELDSWIDKFCLDADVFVLVANSESTLMQTE
Amazon molly       VNQLAHALLQDVDLDAGSLVCVMWPKAKCALLRDDLVLLDS--PGIDVTTELDSWIDKFCLDADVFVLVANSESTLMQTE
Spotted gar        VNQLAHALHQDEHLDAGSLVCVMWPKAKCALLRDDLVLVDS--PGIDVTTELDSWIDKFCLDADVFVLVANSESTLMQTE
Cave fish          VNQLAHALHQDEDLDAGSLVCVMWPKAKCALLRDDLVLVDS--PGIDVTTELDSWIDKFCLDADVFVLVANSESTLMQTE
Zebrafish          VNQLAHALHQDEDLDAGSLVCVMWPKAKCALLRDDLVLVDS--PGIDVTTELDSWIDKFCLDADVFVLVANSESTLMQTE
Coelacanth         VNQLAHALHQNEDLDAGSLVSIMWPSSKCPLLRDDLVLMDS--PGIDVTTELDSWIDRFCLDADVFVLVANSESTLMQTE
Frog               VNQLAHALHQDDLLDSGSLVSVMWPNSKCPLLKDDLVLMDS--PGIDVTTELDSWIDKFCLDADVFVLVANSESTLMQTE
```

```
                     240       250       260       270       280       290       300       310
                   ..|....|....|....|....|....|....|....|....|....|....|....|....|....|....|..
Human              KHFFHKVSERLSRPNIFILNNRWDASASEPEYMEEVRRQHMERCTSFLVDELGVVDRSQAGDRIFFVSAKEVLNARIQKA
Chimpanzee         KHFFHKVSERLSRPNIFILNNRWDASASEPEYMEEVRRQHMERCTSFLVDELGVVDRSQAGDRIFFVSAKEVLNARIQKA
Gorilla            KHFFHKVSERLSRPNIFILNNRWDASASEPEYMEEVRRQHMERCTSFLVDELGVVDRSQAGDRIFFVSAKEVLNARIQKA
Monkey             KHFFHKVSERLSRPNIFILNNRWDASASEPEYMEEVRRQHMERCTSFLVDELGVVDRSQAGDRIFFVSAKEVLNARIQKA
Macaque            KHFFHKVSERLSRPNIFILNNRWDASASEPEYMEEVRRQHMERCTSFLVDELGVVDRSQAGDRIFFVSAKEVLNARIQKA
Marmoset           KHFFHKVSERLSRPNIFILNNRWDASASEPEYMEEVRRQHMERCTSFLVDELGVVDRSQAGDRIFFVSAKEVLNARIQKA
Bushbaby           KQFFHKVSERLSRPNIFILNNRWDASASEPEYMEEVRRQHMERCTSFLVDELGVVDRAQAGDRIFFVSAKEVLNARIQKA
Lemur              KQFFHKVSERLSRPNIFILNNRWDASASEPEYMEEVRRQHMERCSSFLVDELGVVDRAQAGDRIFFVSAKEVLNARIQKA
Gibbon             KHFFHKVSERLSRPNIFILNNRWDASASEPEYMEEVRRQHMERCISFLVDELGVVDRSQAGDRIFFVSAKEVLNARIQKA
Elephant           KQFFHKVSERLSRPNIFILNNRWDASASEPEYMEEVRRQHMERCTGFLVDELGVVDRAQAGDRIFFVSAKEVLNARIQKA
Armadillo          KQFFHKVSERLSRPNIFILNNRWDASASEPEYMEEVRRQHMERCTSFLVDELGVVDRAQAGDRIFFVSAKEVLNARIQKA
Cat                KQFFHKVSERLSRPNIFILNNRWDASASEPEYMEEVRRQHMERCTSFLVDELGVVDRGQAGDRIFFVSAKEVLNARIQKA
Dog                KQFFHKVSERLSRPNIFILNNRWDASASEPEYMEEVRRQHMERCTSFLVDELGVVDRGQAGDRIFFVSAKEVLNARIQKA
Ferret             KQFFHKVSERLSRPNIFILNNRWDASASEPEYMEEVRRQHMERCTSFLVDELGVVDRGQAGDRIFFVSAKEVLNARIQKA
Boar               KQFFHKVSERLSRPNIFILNNRWDASASEPEYMEEVRRQHMERCTSFLVDELGVVDRGQAGDRIFFVSAKEALNARIQKA
Dolphin            KQFFHKVSERLSRPNIFILNNRWDASASEPEYMEEVRRQHMERCTSFLVDELGVVDRGQAGDRIFFVSAKEVLNARIQKA
Sheep              KQFFHKVSERLSRPNIFILNNRWDASASEPEYMEEVRRQHMERCTSFLVDELGVVDRGQAGDRIFFVSAKEVLNARIQKA
Squirrel           KQFFHKVSERLSRPNIFILNNRWDASASEPEYMEEVRRQHMERCTSFLVDELGVVDRAQAGDRIFFVSAKEVLNARIQKA
Guinea pig         KQFFHKVSERLSRPNIFILNNRWDASASEPEYMEEVRRQHMERCTSFLVDELGVVDRAQAGDRIFFVSAKEVLNARIQKA
Rat                KQFFHKVSERLSRPNIFILNNRWDASASEPEYMEEVRRQHMERCTSFLVDELGVVDRAQAGDRIFFVSAKEVLSARVQKA
Mouse              KQFFHKVSERLSRPNIFILNNRWDASASEPEYMEEVRRQHMERCTSFLVDELGVVDRAQAGDRIFFVSAKEVLSARVQKA
Horse              KQFFHKVSERLSRPNIFILNNRWDASASEPEYMEEVRRQHMERCTGFLVDELGVVDRGQAGDRIFFVSAKEVLNARIQKA
Opossum            KQFFHKVSERLSRPNIFILNNRWDASASEPEYMEEVRRQHMERCTSFLVDELGVVDRAQAGDRIFFVSAKEVVNARIQKA
Collrd flyctchr    KQFFHKVNERLSRPNIFILNNRWDASASEPEYMEEVRRQHMERCTSFLVDELGVVDRAQAGDRIFFVSAKEVLNARIQRA
Zebra finch        KQFFHKVNERLSRPNIFILNNRWDASASEPEYMEEVRRQHMERCTGFLVDELGVVDRAQAGDRIFFVSAKEVLNARIQKA
Chicken            KQFFHKVNERLSRPNIFILNNRWDASASEPEYMEEVRRQHMERCTSFLVDELGVVDRTQAGDRIFFVSAKEVLNARIQRA
Turkey             KQFFHKVNERLSRPNIFILNNRWDASASEPEYMEEVRRQHMERCTSFLVDELGVVDRAQAGDRIFFVSAKEVLNARIQKA
Turtle             KQFFHKVNERLSRPNIFILNNRWDASASEPEYMEEVRRQHMERCTSFLVDELGVVDRAQAGDRIFFVSAKEVLNARIQKA
Pufferfish         KSFFHKVNERLSSPNIFILNNRWDASASEPEYMEEVRRQHMDRCSTFLVEELAVVDRAQASDRIFFVSAKEVLQARVQKA
Tilapia            KSFFHKVNERLSSPNIFILNNRWDASASEPEYMEEVRRQHMDRCTNFLVDELGVVDRAQASDRIFFVSAKEVLQARVQKA
Stickleback        KSFFHKVNERLSSPNIFILNNRWDASASEPEYMEEVRRQHMDRCTNFLVDELGVVDRAQASDRIFFVSAKEVLQARVQKA
Cod                KFFFHKVNERLSSPNIFILNNRWDASASEPEYMEEVRRQHMDRCSSFLVDELGVVDRAQASDRIFFVSAKEVLQARIQKA
Platyfish          KSFFHKVNQRLSSPNVFILNNRWDASASEPEYMEEVRRQHMDRCTNFLVDELGVVDRAQASDRIFFVSAKEVLQARVQKA
Amazon molly       KSFFHKVNQRLSSPNVFILNNRWDASASEPEYMEEVRRQHMDRCTNFLVDELGVVDRAQASDRIFFVSAKEVLQARVQKA
Spotted gar        KQFFHKVNERLSRPNIFILNNRWDASASEPEYMEEVRHQHMDRCTSFLVDELAVVDRAQASDRIFFVSAKEVLQARIQKA
Cave fish          KSFFHKVNERLSSPNIFILNNRWDASASEPEYMEEVRRQHMDRCSSFLVDELGVVDRAQASDRIFFVSAKEVLQARVQKA
Zebrafish          KSFFHKVNERLSSPNIFILNNRWDASANEPEYMEEVRRQHMDRCTSFLVDELRVVDRSHAGDRIFFVSAKEVLQARVQKA
Coelacanth         KQFFHKVNERLSRPNIFILNNRWDASASEPEYMEEVRRQHMDRCTSFLVDELGVVDRAQAGDRIFFVSAKEVLNARIQKA
Frog               KQFFHKVNERLSRPNIFILNNRWDASASEPEYMEEVS-IHTFRIHATLPYFVPLLKKAHVQARLKFAN--EHLNDSVTLP
```

```
                  320       330       340       350       360       370       380       390
Human             QGMPEGGGALAEGFQVRMFEFQNFERRFEECISQSAVKTKFEQHTVRAKQIAEAVRLIMDSLHMAAREQQVYCEEMREER
Chimpanzee        QGMPEGGGALAEGFQVRMFEFQNFERRFEECISQSAVKTKFEQHTVRAKQIAEAVRLIMDSLHVAAREQQVYCEEMREER
Gorilla           QGMPEGGGALAEGFQVRMFEFQNFERRFEECISQSAVKTKFEQHTVRAKQIAEAVRLIMDSLHVAAREQQVYCEEMREER
Monkey            QGMPEGGGALAEGFQVRMFEFQNFERRFEECISQSAVKTKFEQHTVRAKQIAEAVRLIMDSLHVAAREQQVYCEEMREER
Macaque           QGMPEGGGALAEGFQVRMFEFQNFERRFEECISQSAVKTKFEQHTVRAKQIAEAVRLIMDSLHVAAREQQVYCEEMREER
Marmoset          QGMPEAGGALAEGFQVRMFEFQNFERRFEECISPLAVKTKFEQHTVRAKQIAEAVRLIMDSLHVAAREQQVYCEEMREER
Bushbaby          QGMPEGGGALAEGFQVRMFEFQNFERRFEECISQSAVKTKFEQHTVRAKQIAEAVRLIMDSLHIAAQEQRVYCLEMREER
Lemur             QGMPEGGGALAEGFQVRMFEFQNFERRFEECISQSAVKTKFEQHTVRAKQIAEAVRFIMDSLHIAAQEQRVYCLEMREER
Gibbon            QGMPEGGGALAEGFQVRMFEFQNFERRFEECISQSAVKTKFEQHTVRAKQIAEAVRLIMDSLHVAAREQQVHAETPCQKK
Elephant          QGMPEGGGALAEGFQVRMFEFQNFERRFEECISQSAVKTKFEQHTVRAKQIAEAVRLIMDSLHIAAQEQRVYCLEMREER
Armadillo         QGMPEGGGALAEGFQVRMFEFQNFERRFEECISQSAVKTKFEQHTVRAKQIAEAVRLIMDSLHVAAQEQRVYCLEMREER
Cat               QGMPEGGGALAEGFQVRMFEFQNFERRFEECISQSAVKTKFEQHTVRAKQIAEAVRLIMDSLHVAAQEQRVYCLEMREER
Dog               QGMPEGGGALAEGFQVRMFEFQNFERRFEECISQSAVKTKFEQHTVRAKQIAEAVRLIMDSLHIAAQEQRVYCLEMREER
Ferret            QGMPEGGGALAEGFQVRMFEFQNFERRFEECISQSAVKTKFEQHTVRAKQIAEAVRLIMDSLHIAAQEQRVYCLEMREER
Boar              QGMPEGGGALAEGFQVRMFEFQNFERRFEECISQSAVKTKFEQHTVRAKQXAEAVRLIMDSLHIAAQEQRVYCLETREER
Dolphin           QGMPEGGGALAEGFQVRMFEFQNFERRFEECISQSAVKTKFEQHTVRAKQIAEAVRLIMDSLHIAAQEQRVYCLEMREER
Sheep             QGMPEGGGALAEGFQVRMFEFQNFERRFEECISQSAVKTKFEQHTVRAKQIAEAVRLIMDSLHIAAQEQRVYCLETREER
Squirrel          QGMPEGGGALAEGFQVRMFEFQNFERRFEECISQSAVKTKFEQHTVRAKQIAEAVRFIMDSLHIAAQEQRVYCLEMREER
Guinea pig        QGMPEGGGALAEGFQVRMFEFQNFERRFEECISQSAVKTKFEQHTVRAKQIAEAVRLIMDSLHIAAQEQRVYCQEMREER
Rat               QGMPEGGGALAEGFQVRMFEFQNFERRFEECISQSAVKTKFEQHTVRAKQIAEAVRLIMDSLHIAAQEQRVYCLEMREER
Mouse             QGMPEGGGALAEGFQVRMFEFQNFERQFEECISQSAVKTKFEQHTVRAKQIAEAVRLIMDSLHIAAQEQRVYCLEMREER
Horse             QGMPEGGGALAEGFQVRMFEFQNFERRFEECISQSAVKTKFEQHTVRAKQIAEAVRLIMDSLHIAAQEQRVYCLEMREER
Opossum           QGMPEGGGALAEGFQVRMFEFQNFERRFEECISQSAVKTKFEQHTVRAKQMVEDARLIMDSVHVAAQEQRVYCQETREER
Collrd flyctchr   QGMPEGGGALADGFQVRMLEFQSFERRFEECISQSAVKTKFEQHTVRAKQIAEDVRLIMDSVHVSAQEQRVYCLEMREER
Zebra finch       QGMPEGGGALADGFQVRMLEFQSFERRFEECISQSAVKTKFEQHTVRAKQIAEDVRLIMDSVHVAAQEQRVYCLEMREER
Chicken           QGMPEGGGALADGFQVRMFEFQNFERRFEECISQSAVKTKFEQHTVRAKQIAEDVRLIMDSVHVAAQEQRVYCLEMREER
Turkey            QGMPEGGGALADGFQVRMFEFQNFERRFEECISQSAVKTKFEQHTVRAKQIAEDVRLIMDSVHVAAQEQRVYCLEMREER
Turtle            QGMPEGGGALAEGFQVRMFEFQNFERRFEECISQSAVKTKFEQHTVRAKQIAEDVRLIMDSLHIAAQEQRVYCLEMREER
Pufferfish        QGMPEAGGALAEGFQARMFEFQNFERRFEECISQSAVKTKFEQHTVRAKQISEALRHIMDSVHVAAQEQTVYCLETKEER
Tilapia           QGMPEAGGALAEGFQARMFEFQNFERRFEECISQSAVKTKFEQHTVRAKQISEALRHIMDSVYIAAQEQRVYCLETKEDR
Stickleback       QGMPEAGGALAEGFQARMFEFQNFERRFEECISQSAVKTKFEQHTVRAKQISEALRRIMDSVHIAAQEQRIYCLETKEDR
Cod               QGMPEAGGALAEGFQARMFEFQNFERRFEECISQSAVKTKFEQHTVRAKQISEALRLIMDSVHVATQEQRIHCMETREDR
Platyfish         QGMPESGGALAEGFQARMFEFQNFERRFEECISQSAVKTKFEQHTVRAKQISEALRHIMDLVHVAAQEQRLYCLETKEDR
Amazon molly      QGMPESGGALAEGFQARMFEFQNFERRFEECISQSAVKTKFEQHTVRAKQISEALRRIMDLVHVAAQEQRLYCLETKEDR
Spotted gar       QGMPEGGGALAEGFQARMFEFQNFERRFEECISQSAVKTKFEQHTVRAKQISETLRQIMDSVHIAAQEQRVHCMETREER
Cave fish         QGMPEAGGALAEGFQARMFEFQNFERRFEECISQSAVKTKFEQHTVRAKQISEALRLIMDSVHVAAQEQRIHCMETKEER
Zebrafish         QGMPEAGGALAEGFQARMFEFQNFERRFEECISQSAVKTKFEQHTTRAKQISEALRLIMDSVHIAAQEQRIHCLEMKEER
Coelacanth        QGMPEGGGALAEGFQARMFEFQNFERRFEECISQSAVKTKFEQHTVRAKQISEALRQIMDSVHVSAQEQRVHCLETREDR
Frog              YYPALLGGALAEGFQARMFEFQNFERRFEECISQSAVKTKFEQHTKRAKQIAEVLRQIMESVHVAAQEQRCLCLEKREEF
```

```
                  400       410        420       430       440       450       460       470
Human             QDRLKFIDKQLELLAQDYKLR-IKQITEEVERQVSTAMAEEIRRLSVLVDDYQMDFHPSPVVLKVYKNELHRHIEEGLGR
Chimpanzee        QDRLKFIDKQLELLAQDYKLR-IKQITEEVERQVSTAMAEEIRRLSVLVDDYQMDFHPSPVVLKVYKNELHRHIEEGLGR
Gorilla           QDRLKFIDKQLELLAQDYKLR-IKQITEEVERQVSTAMAEEIRRLSVLVDDYQMDFHPSPVVLKVYKNELHRHIEEGLGR
Monkey            QDRLKFIDKQLELLAQDYKLR-IKQITEEVERQVSTAMAEEIRRLSVLVDDYQMDFHPSPVVLKVYKNELHRHIEEGLGR
Macaque           QDRLKFIDKQLELLAQDYKLR-IKQITEEVERQVSTAMAEEIRRLSVLVDDYQMDFHPSPVVLKVYKNELHRHIEEGLGR
Marmoset          QDRLKFIDKQLELLAQDYKLR-IKQITEEVERQVSTAMAEEIRRLSVLVDDYQMDFHPSPVVLKVYKNELHRHIEEGLGR
Bushbaby          QDRLRFIDKQLELLAQDYKLR-IKQITEEVERQVSTAMAEEIRRLSVLVDEYQMDFHPSPVVLKVYKNELHRHIEEGLGR
Lemur             QDRLRFIDKQLELLAQDYKLR-IKQITEEVERQVSTAMAEEIRRLSVLVDEYQMDFHPSPVVLKVYKNELHRHIEEGLGR
Gibbon            KKKFHFCDYYAWLASGPCHLRGFNSIEELRRLLVSTAMAEEIRRLSVLVDDYQMDFHPSPVVLKVYKNELHRHIEEGLGR
Elephant          QDRLSFIDKQLELLAQDYKLR-IKQITEEVERQVSTAMAEEIRRLSVLVDEYQMDFHPSPVVLKVYKNELHRHIEEGLGR
Armadillo         QDRLRFIDKQLELLAQDYKLR-IKQITEEVERQVSTAMAEEIRRLSVLVDEYQMDFHPSPVVLKVYKNELHRHIEEGLGR
Cat               QERLRFIDKQLELLAQDYKLR-IKQITEEVERQVSTAMAEEIRRLSVLVDEYQMDFHPSPVVLKVYKNELHRHIEEGLGR
Dog               QERLRFIDKQLELLAQDYKLR-IKQITEEVERQVSTAMAEEIRRLSVLVDDYQMDFHPSPVVLKVYKNELHRHIEEGLGR
Ferret            QERLRFIDKQLELLAQDYKLR-IKQITEEVERQVSTAMAEEIRRLSVLVDEYQMDFHPSPVVLKVYKNELHRHIEEGLGR
Boar              QERLRFIDKQLELLAQDYKLR-IKQITEEVERQVSTAMAEEIRRLSVLVDEYQMDFHPSPVVLKVYKNELHRHIEEGLGR
Dolphin           QERLRFIDKQLELLAQDYKLR-IKQITEEVERQVSTAMAEEIRRLSVLVDEYQMDFHPSPVVLKVYKNELHRHIEEGLGR
Sheep             QERLRFIDKQLELLAQDYKLR-IKQITEEVERQVSTAMAEEIRRLSVLVDEYQMDFHPSPVVLKVYKNELHRHIEEGLGR
Squirrel          QDRLRFIDKQLELLAQDYKLR-IKQITEEVERQVSTAMAEEIRRLSVLVDEYQMDFHPSPVVLKVYKNELHRHIEEGLGR
Guinea pig        QDRLRFIDKQLELLAQDYKLR-IKQITEEVERQVSTAMAEEIRRLSVLVDEYQMDFHPSPVVLKVYKNELHRHIEEGLGR
Rat               QDRLRFIDKQLELLAQDYKLR-IKQMTEEVERQVSTAMAEEIRRLSVLVDEYQMDFHPSPVVLKVYKNELHRHIEEGLGR
Mouse             QDRLRFIDKQLELLAQDYKLR-IKQITEEVERQVSTAMAEEIRRLSVLVDEYQMDFHPSPVVLKVYKNELHRHIEEGLGR
Horse             QERLRFIDKQLELLAQDYKLR-IKQITEEVERQVSTAMAEEIRRLSVLVDEYQMDFHPSPVVLKVYKNELHRHIEEGLGR
Opossum           QERLGFIDKQLELLTQDFKVR-IKQITEEVERQVSNAMAEEIRRLSVLVDEYQMDFHPSPVVLKVYKNELHRHIEEGLGR
Collrd flyctchr   QDRLGFIDKQLELLTQDYKRK-IKQITEEVERQVSNAMAEEIRRLSVLVDEYQADFHPSQVVLKVYKSELHKHIEEGLGR
Zebra finch       QDRLGFIDKQLELLTQDYKRK-IKQITEEVERQVSNAMAEEIRRLSVLVDEYQADFHPSQVVLKVYKSELHKHIEEGLGR
Chicken           QERLGFIDKQLELLTQDYKRK-IKQITEEVERQVSNAMAEEIRRLSVLVDEYQADFHPSQVVLKVYKNELHKHIEEGLGR
Turkey            QERLGFIDKQLELLTQDYKRK-IKQITEEVERQVSNAMAEEIRRLSVLVDEYQADFHPSQVVLKVYKNELHKHIEEGLGR
Turtle            QERLGFIDKQLELLTQDYKGK-IKQITEEVERQVSNAMAEEIRRLSVLVDDYQMDFHPSPVVLKVYKNELHRHIEEGLGR
Pufferfish        QERLEFIDKQLDLLTLDSKAK-IRKITEEVERQVSNAMAEEIRKLHLLVDDFHMEFHPSSVVLKVYKNELHRHVEEGLGK
Tilapia           QDRLEFIDKQLDLLTLDSKSK-IKKITEEVERQVSNAMADEIRKLHVLVDDFHMDFHPSPVVLKVYKNELHRHIEEGLGK
Stickleback       QDRLEFIDKQLDLLSMDCKSK-IKKITEEVERQVSNAMSEEIRKLHVLVDDYHMDFHPSPVVLKVYKNELHRHIEVGLGK
Cod               QDRMEFIDKQLDLLSMDCKAK-IKKITEEVERQVSNAMAEEIRRLYVLVDDFHMDFHPSPVVLKVYKNELHRHIEEGLGR
Platyfish         QQRLEFIEKQLDLLTMDCKAK-IKRITEEVERQVTNTMAEEIRKLHVLVDDFHMDFHPSPVVLKVYKNELHRYIEDGLGK
Amazon molly      QQRLEFIEKQLDLLTMDCKAK-IKRITEDVERQVTNTMAEEIRKLHVLVDDFHMDFHPSPVVLKVYKNELHRHIEDGLGK
Spotted gar       QDRLEFIDKQLDLLTLDCKSK-IKQITEEVERQVSNAMAEEIRRLYVLVDDFHMDFHPSQVVLKVYKNELHKHIEEGLGR
Cave fish         EDRLDFIDKQLDLLTLDCKSK-IRKITEEVEKQVSNAMAEEIRRLHVLVDEFHLDFHPSQVVLKVYKNELHRHIEEGLGR
Zebrafish         EDRLEFIDKQLDLLTLDCKSK-IKKITEEVEKQVSNAMAEEIRRLAVLVDDFHMDFHPSPVVLKVYKNELHRHIEEGLGR
Coelacanth        QDRLEFIEKQLDLLSQECKRK-IKQITEEVEKQVSNAMAEEIRRLSVLVDDFQMDFHPSPVVVKVYKNELHRHIEEGLGR
Frog              RDRLEFIEKQLELLTEDYKFK-IKQITDEVERQVSNAMAEEIRRLSILVDEFQLDFHPSSVVLKVYKNELHRHIEEGLGR
```

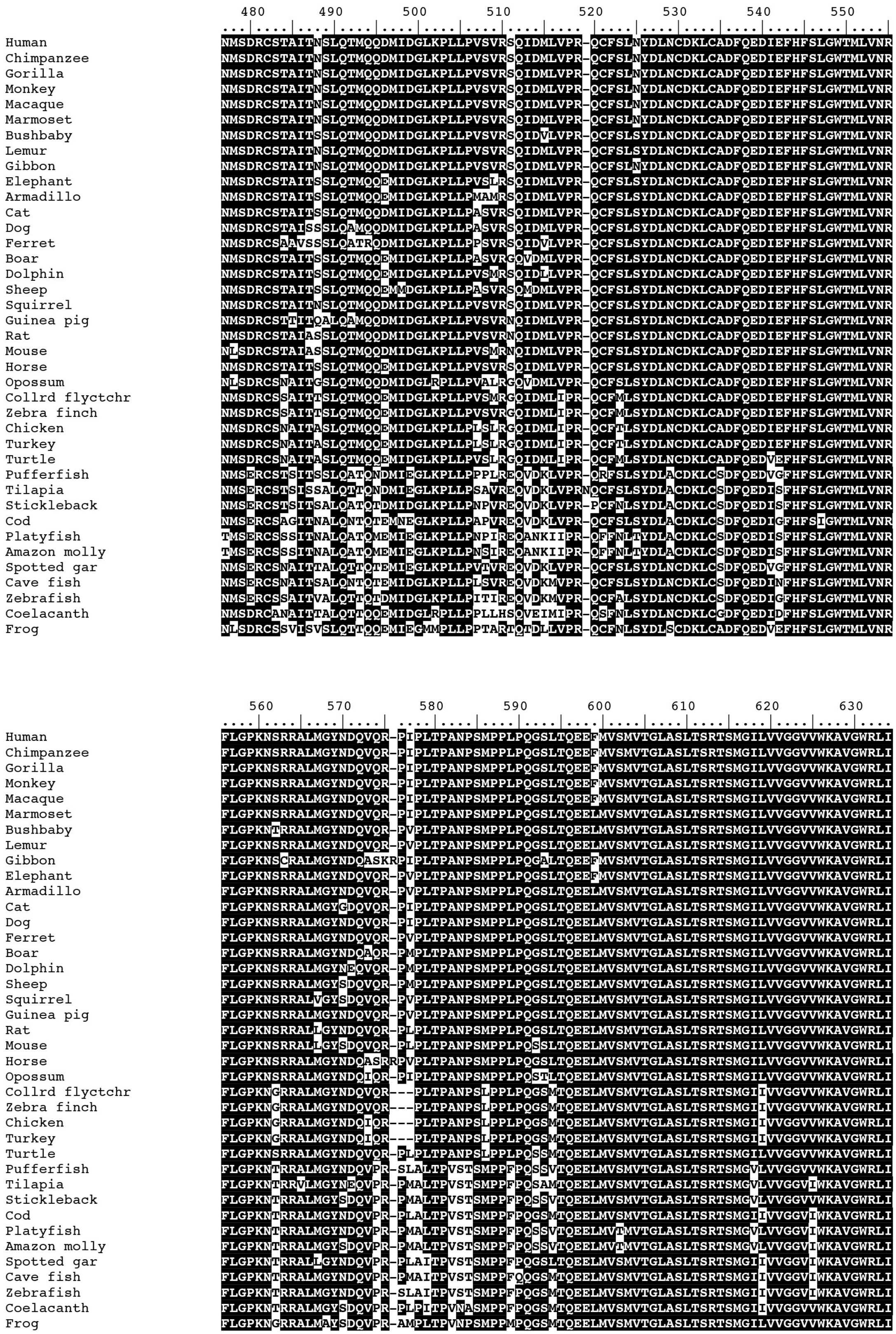

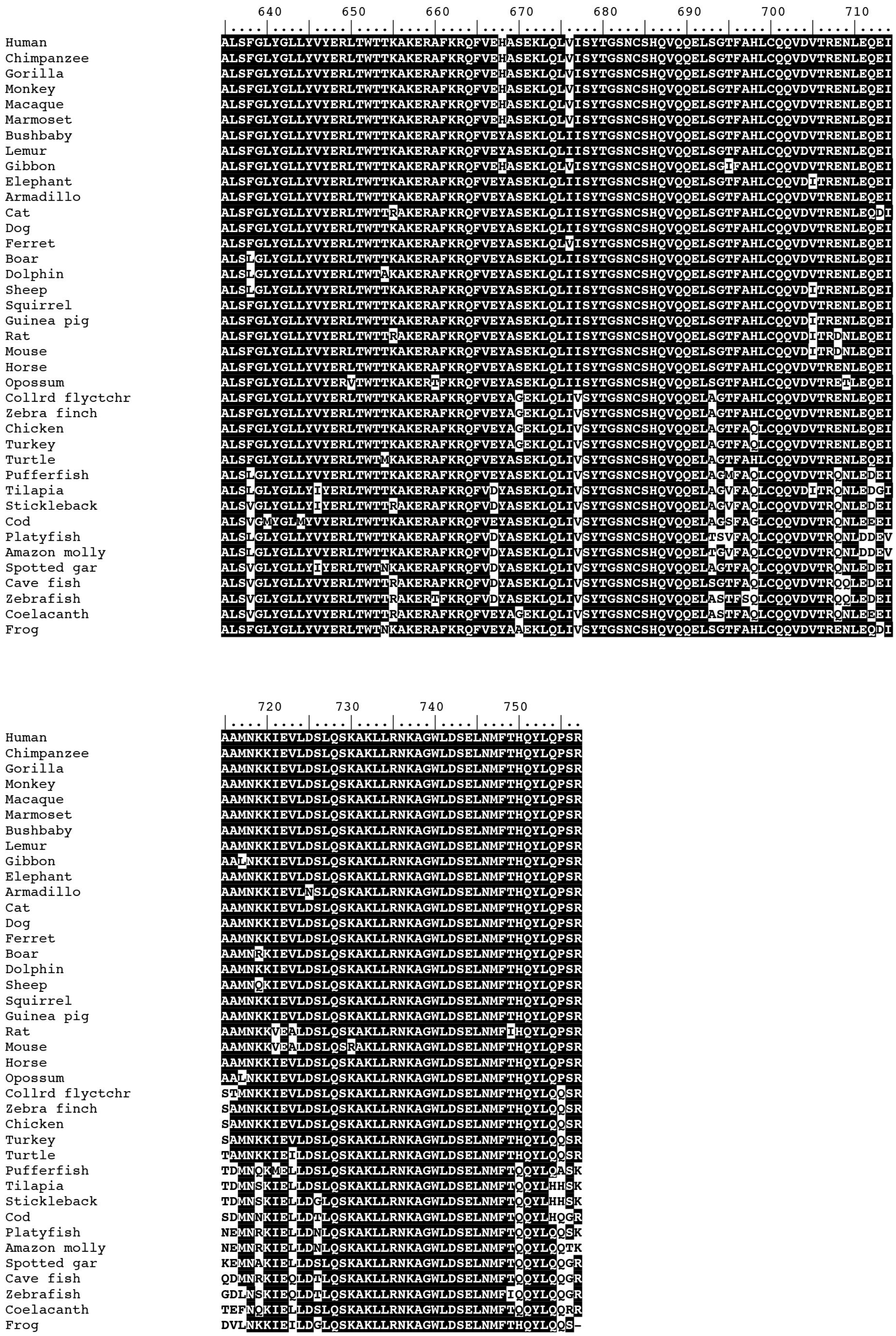

Fig. S2. *Multi-species alignment of Mfn2 amino acid sequence.* Black highlighting shows identity with human Mfn2 protein.

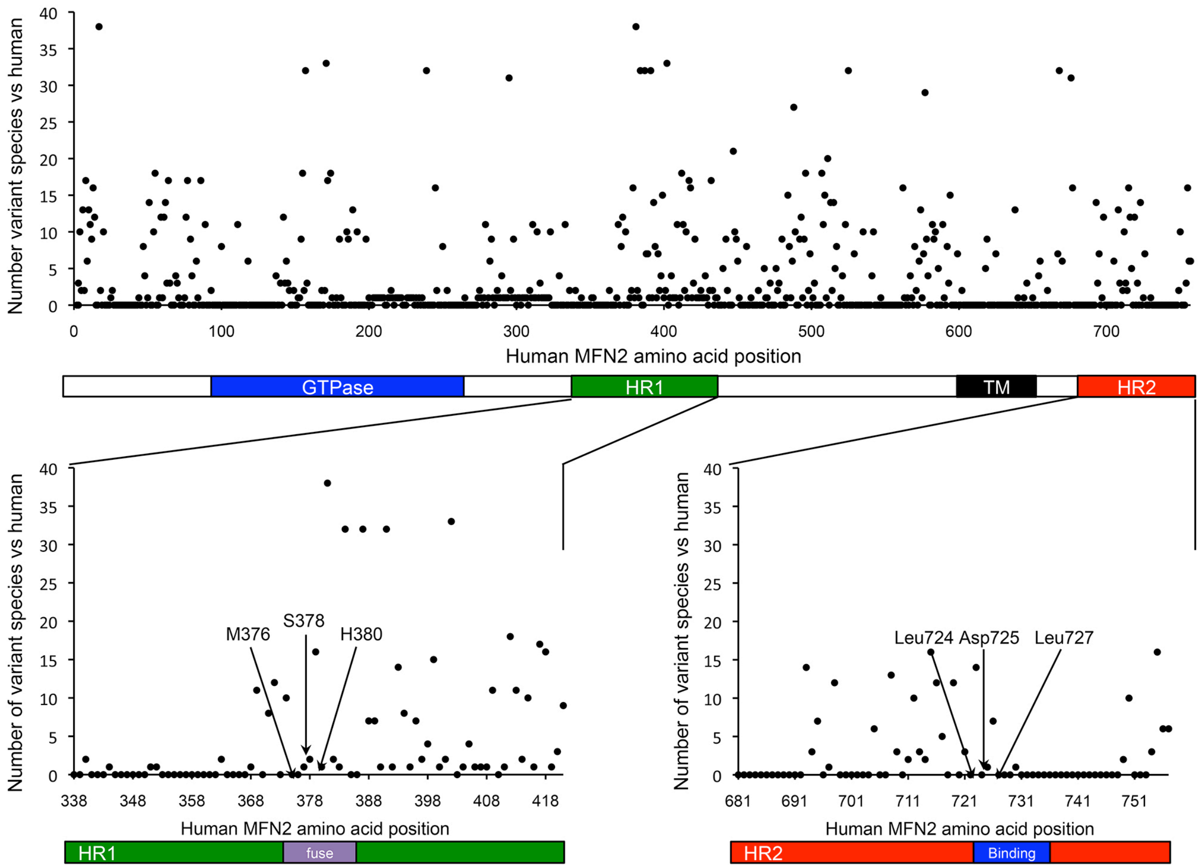

Fig. S3. *Homology plot of Mfn2 amino acid sequence by functional domain.* Positions of HR1 MP374-384 ("fuse") and its HR2 interacting site ("Binding") are shown on exploded views below.

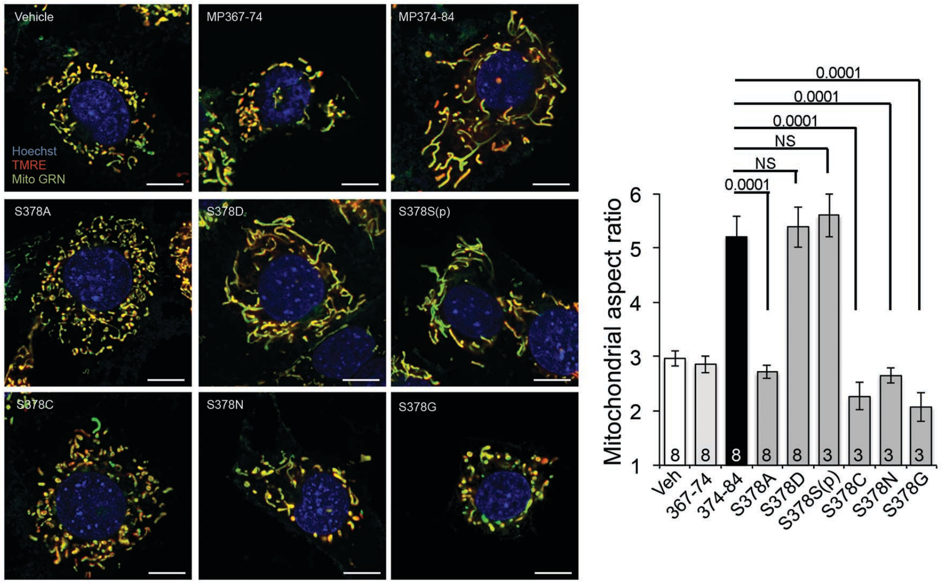

Fig. S4. *Mfn2 Ser378 charge status determines fusion-promoting activity of HR1 MP374-384.* Ser378 substitution analysis of mitochondrial fusion promoted by HR1 MP374-384. Representative confocal images of MitoTracker Green/TMRE (red) stained live Mfn2-/- (Mfn2 knockout) MEFs are on the left; scale bars are 10 μm. Group mean data from Figure 1D are to the right; p values are by ANOVA with Tukey's post hoc comparison.

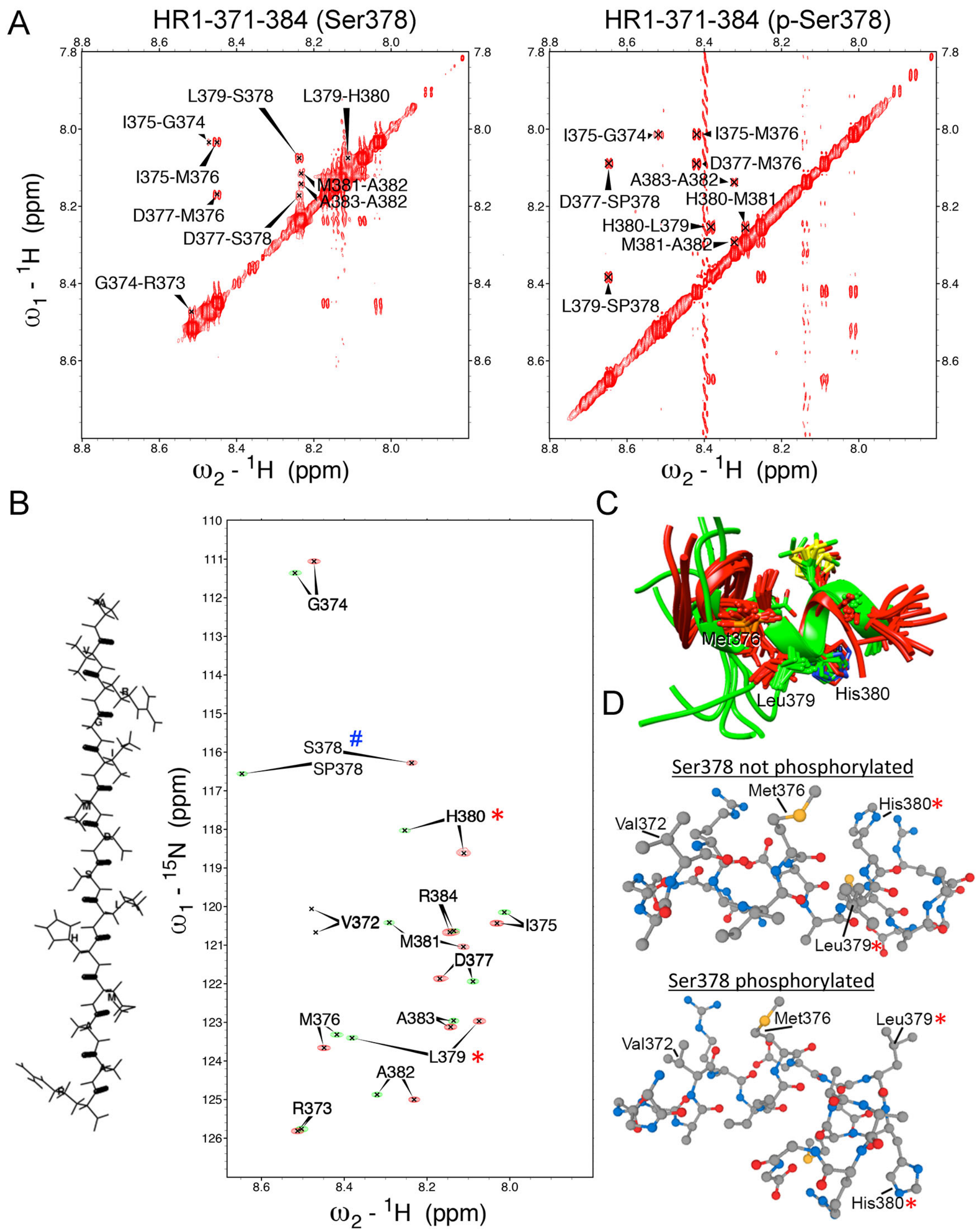

Fig. S5. *NMR spectroscopy suggests a structural mechanism for effects of Ser378 phosphorylation on HR1 372-384 minipeptide fusogenic function.* **(A)** Amide proton regions of 2D NOESY spectra of Ala371 to Arg384 fragment of hMfn2. *left* – unphosphorylated Ser378 peptide; *right* – peptide synthesized with phosphorylated Ser-378. Sequential cross peaks between amide groups indicative of α-helical secondary structure are labeled. **(B)** Overlaid ^{15}N-^{1}H heteronuclear single quantum coherence spectra of minipeptide backbone amides (bold highlights on covalent wire-model to the left). Red is Ser378 peptide; green is (p)-Ser378 peptide. # marks the positions of Ser378 and (p)-Ser378. In addition to Ser378, the amide signals for amino acids 379-382 shifted down-field (i.e. to higher values) after phosphorylation, as observed when amides within peptides form or strengthen hydrogen bonds. Here, phosphorylation of Ser378 can induce hydrogen bonding for the amide of Leu379, stabilizing the downstream helix and evoking the observed down-field shifts for amides of His380 and Met381. **(C)** Ensembles of structures calculated from NMR restraints. Color coding is the same as in (B). **(D)** PepFold3 modeling of the HR1 minipeptide shows how different backbone structure provoked by Ser378 phosphorylation (see panel B) can alter Leu379 and His 380. * in (B) and (D) mark amino acids with the greatest changes between Ser378 and (p)-Ser378 peptides.

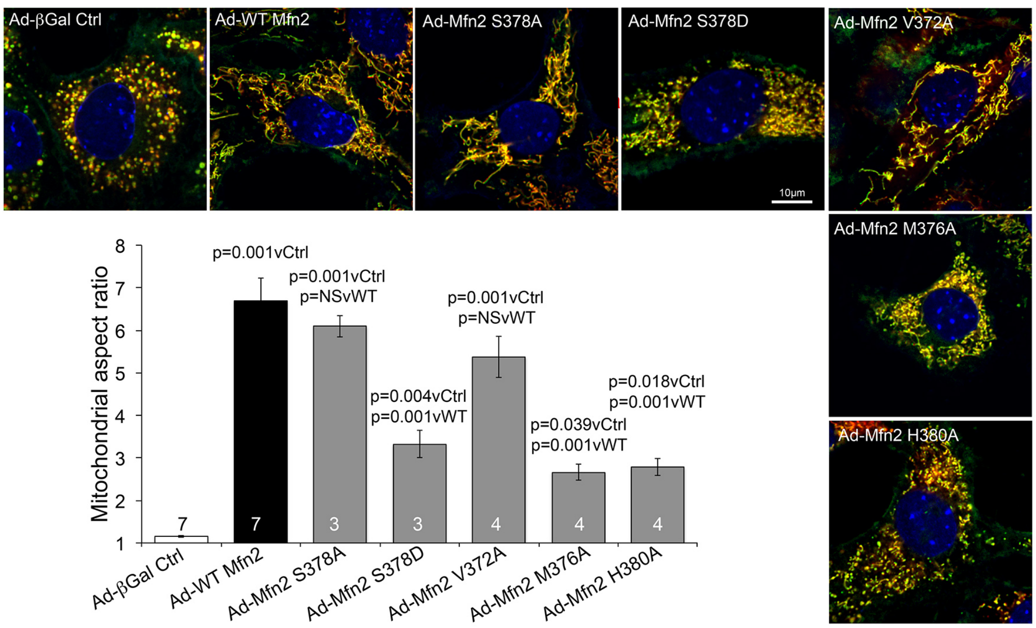

Fig S6. *Mutagenesis analysis of Mfn2-function based on Ser378 phosphorylation status and integrity of Met376 and His380 that are spatially regulated by Ser378 phosphorylation.* Group data and representative confocal images showing mitochondrial aspect ratio in mitofusin deficient cells (Mfn1-/-, Mfn2-/- double knockout MEFs) infected with adnoviri expressing β-galactosidase (negative control), wild-type (WT) Mfn2 (positive control), or different single amino acid Mfn2 mutants. Fusogenic function was impaired in pseudo-phosphorylated Mfn2 Ser378Asp (S378D) and alanine-substituted Mfn2 Met376Ala (M376A) and His380Ala (H380A); non-phosphorylatable Mfn2 Ser378Ala (S378A) and Mfn2 Val372Ala (V372A, which is not in the HR1-HR2 interacting domain) retained full activity. p values are by ANOVA with Tukey's post hoc comparison. MEFs were stained as described in Fig. S4 legend. Scale bar is 10 μm.

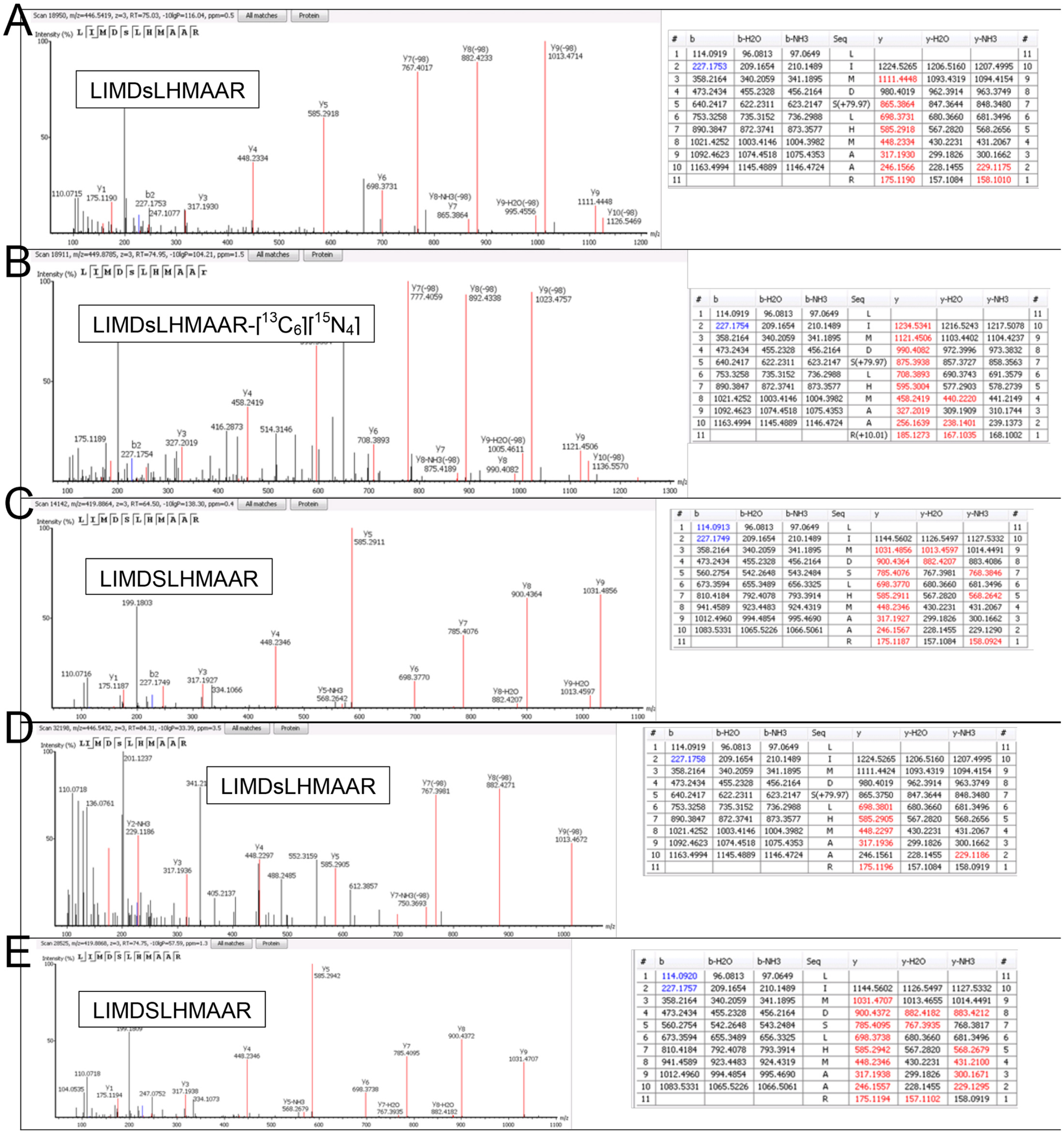

Fig. S7. *High-resolution tandem mass spectra of peptides from a tryptic digest of PINK1-treated recombinant human Mfn2*. The spectra of the phosphopeptide with the Ser-378 phosphorylation site **(A)**, a stable isotope-labeled synthetic phosphopeptide **(B)**, and the non-phosphorylated peptide **(C)** are shown from a 4-hour in vitro PINK1 phosphorylation experiment. **(D)** and **(E)** are like (A) and (C) after an overnight period for PINK1 phosphorylation. The m/z values for the assigned ions are highlighted in the adjacent ion tables.

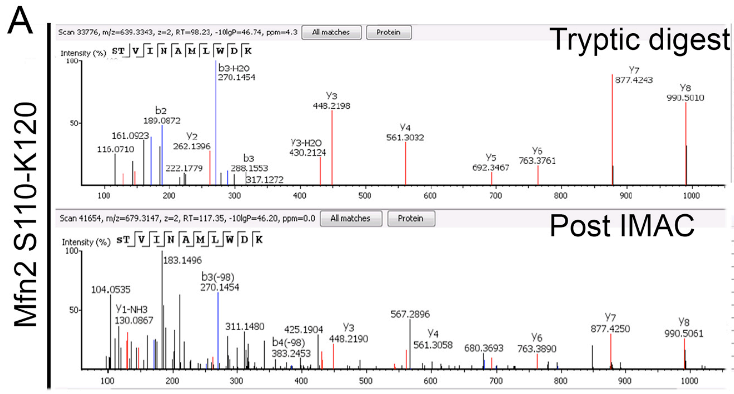

#	b	b-H2O	b-NH3	b (2+)	Seq	y	y-H2O	y-NH3	y (2+)	#
1	88.0399	70.0293	71.0129	44.5199	S					11
2	189.0872	171.0765	172.0605	95.0438	T	1190.6238	1172.6133	1173.5968	595.8119	10
3	288.1553	270.1454	271.1290	144.5780	V	1089.5760	1071.5656	1072.5491	545.2880	9
4	401.2400	383.2294	384.2130	201.1200	I	990.5010	972.4971	973.4807	495.7538	8
5	515.2830	497.2724	498.2560	258.1415	N	877.4243	859.4131	860.3967	439.2118	7
6	586.3201	568.3095	569.2931	293.6600	A	763.3761	745.3701	746.3537	382.1903	6
7	717.3605	699.3500	700.3336	359.1803	M	692.3467	674.3330	675.3166	346.6718	5
8	830.4446	812.4340	813.4176	415.7223	L	561.3032	543.2925	544.2761	281.1516	4
9	1016.5239	998.5134	999.4969	508.7620	W	448.2198	430.2124	431.1920	224.6095	3
10	1131.5509	1113.5404	1114.5239	566.2755	D	262.1396	244.1292	245.1127	131.5699	2
11					K	147.1125	129.1027	130.0858	74.0564	1

#	b	b-H2O	b-NH3	b (2+)	Seq	y	y-H2O	y-NH3	y (2+)	#
1	168.0062	149.9956	150.9792	84.5031	S(+79.97)					11
2	269.0538	251.0433	252.0268	135.0269	T	1190.6238	1172.6133	1173.5968	595.8119	10
3	368.1223	350.1117	351.0953	184.5611	V	1089.5829	1071.5656	1072.5491	545.2880	9
4	481.2063	463.1958	464.1794	241.1032	I	990.5061	972.4971	973.4807	495.7538	8
5	595.2493	577.2387	578.2223	298.1246	N	877.4250	859.4131	860.3967	439.2118	7
6	666.2864	648.2758	649.2594	333.6432	A	763.3890	745.3701	746.3537	382.1903	6
7	797.3268	779.3163	780.2999	399.1634	M	692.3446	674.3330	675.3166	346.6718	5
8	910.4109	892.4003	893.3839	455.7054	L	561.3058	543.2982	544.2942	281.1516	4
9	1096.4902	1078.4797	1079.4633	548.7451	W	448.2190	430.2124	431.2044	224.6095	3
10	1211.5172	1193.5067	1194.4902	606.2586	D	262.1404	244.1292	245.1127	131.5699	2
11					K	147.1131	129.1028	130.0867	74.0564	1

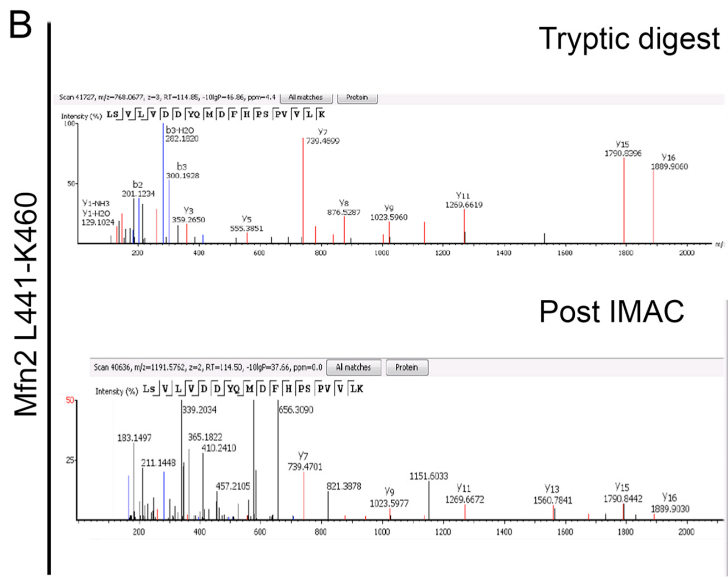

#	b	b-H2O	b-NH3	b (2+)	Seq	y	y-H2O	y-NH3	y (2+)	#
1	114.0919	96.0813	97.0649	57.5459	L					20
2	201.1234	183.1125	184.0969	101.0620	S	2189.0947	2171.0842	2172.0676	1095.0474	19
3	300.1928	282.1820	283.1653	150.5962	V	2102.0627	2084.0522	2085.0356	1051.5314	18
4	413.2760	395.2658	396.2494	207.1382	L	2002.9943	1984.9838	1985.9673	1001.9993	17
5	512.3448	494.3342	495.3178	256.6724	V	1889.9060	1871.8997	1872.8832	945.4551	16
6	627.3717	609.3611	610.3447	314.1859	D	1790.8396	1772.8313	1773.8148	895.9209	15
7	742.3987	724.3881	725.3717	371.6993	D	1675.8148	1657.8043	1658.7878	838.4182	14
8	905.4620	887.4514	888.4350	453.2310	Y	1560.7878	1542.7773	1543.7609	780.8901	13
9	1033.5205	1015.5099	1016.4935	517.2603	Q	1397.7245	1379.7140	1380.6975	699.3622	12
10	1164.5610	1146.5505	1147.5341	582.7805	M	1269.6619	1251.6555	1252.6390	635.3330	11
11	1279.5880	1261.5775	1262.5610	640.2940	D	1138.6218	1120.6150	1121.5985	569.8127	10
12	1426.6564	1408.6459	1409.6294	713.8282	F	1023.5960	1005.5880	1006.5715	512.2993	9
13	1563.7153	1545.7048	1546.6884	782.3577	H	876.5287	858.5196	859.5032	438.7651	8
14	1660.7681	1642.7576	1643.7411	830.8840	P	739.4699	721.4606	722.4442	370.2356	7
15	1747.8000	1729.7896	1730.7731	874.4000	S	642.4185	624.4079	625.3915	321.7092	6
16	1844.8529	1826.8424	1827.8259	922.9265	P	555.3851	537.3759	538.3594	278.1932	5
17	1943.9213	1925.9108	1926.8943	972.4606	V	458.3337	440.3231	441.3067	229.6668	4
18	2042.9897	2024.9792	2025.9628	1021.9949	V	359.2650	341.2547	342.2383	180.1326	3
19	2156.0737	2138.0632	2139.0466	1078.5369	L	260.1986	242.1863	243.1698	130.5984	2
20					K	147.1130	129.1024	130.0866	74.0564	1

#	b	b-H2O	b-NH3	b (2+)	Seq	y	y-H2O	y-NH3	y (2+)	#
1	114.0919	96.0813	97.0649	57.5459	L					20
2	281.0902	263.0797	264.0632	141.0451	S(+79.97)	2269.0610	2251.0505	2252.0339	1135.0305	19
3	380.1586	362.1481	363.1317	190.5793	V	2102.0627	2084.0522	2085.0356	1051.5314	18
4	493.2427	475.2321	476.2157	247.1214	L	2002.9943	1984.9838	1985.9673	1001.9971	17
5	592.3111	574.3005	575.2841	296.6555	V	1889.9030	1871.8997	1872.8832	945.4640	16
6	707.3381	689.3275	690.3111	354.1690	D	1790.8442	1772.8313	1773.8148	895.9209	15
7	822.3650	804.3544	805.3380	411.6825	D	1675.8282	1657.8043	1658.7878	838.4074	14
8	985.4283	967.4178	968.4014	493.2142	Y	1560.7841	1542.7773	1543.7609	780.8939	13
9	1113.4869	1095.4764	1096.4600	557.2435	Q	1397.7245	1379.7140	1380.6975	699.3622	12
10	1244.5273	1226.5168	1227.5004	622.7637	M	1269.6672	1251.6555	1252.6390	635.3330	11
11	1359.5543	1341.5438	1342.5273	680.2772	D	1138.6270	1120.6150	1121.5985	569.8127	10
12	1506.6227	1488.6122	1489.5957	753.8113	F	1023.5977	1005.5880	1006.5715	512.2993	9
13	1643.6816	1625.6711	1626.6547	822.3408	H	876.5280	858.5196	859.5032	438.7651	8
14	1740.7344	1722.7239	1723.7074	870.8672	P	739.4701	721.4606	722.4442	370.2356	7
15	1827.7665	1809.7560	1810.7395	914.3832	S	642.4185	624.4079	625.3915	321.7092	6
16	1924.8192	1906.8087	1907.7922	962.9096	P	555.3871	537.3759	538.3594	278.1932	5
17	2023.8876	2005.8771	2006.8606	1012.4438	V	458.3337	440.3231	441.3067	229.6668	4
18	2122.9561	2104.9456	2105.9290	1061.9780	V	359.2653	341.2547	342.2383	180.1326	3
19	2236.0400	2218.0295	2219.0129	1118.5200	L	260.1967	242.1863	243.1698	130.5984	2
20					K	147.1128	129.1022	130.0858	74.0564	1

Fig. S8. *High-resolution mass spectra of PINK1-phosphorylated recombinant human Mfn2 demonstrating phosphorylation of Thr111* ***(A)*** *and Ser442* ***(B)***. These spectra were obtained in the study shown in Fig. S7D and E. *m/z* values for assigned fragmentation ions are shown to the right.

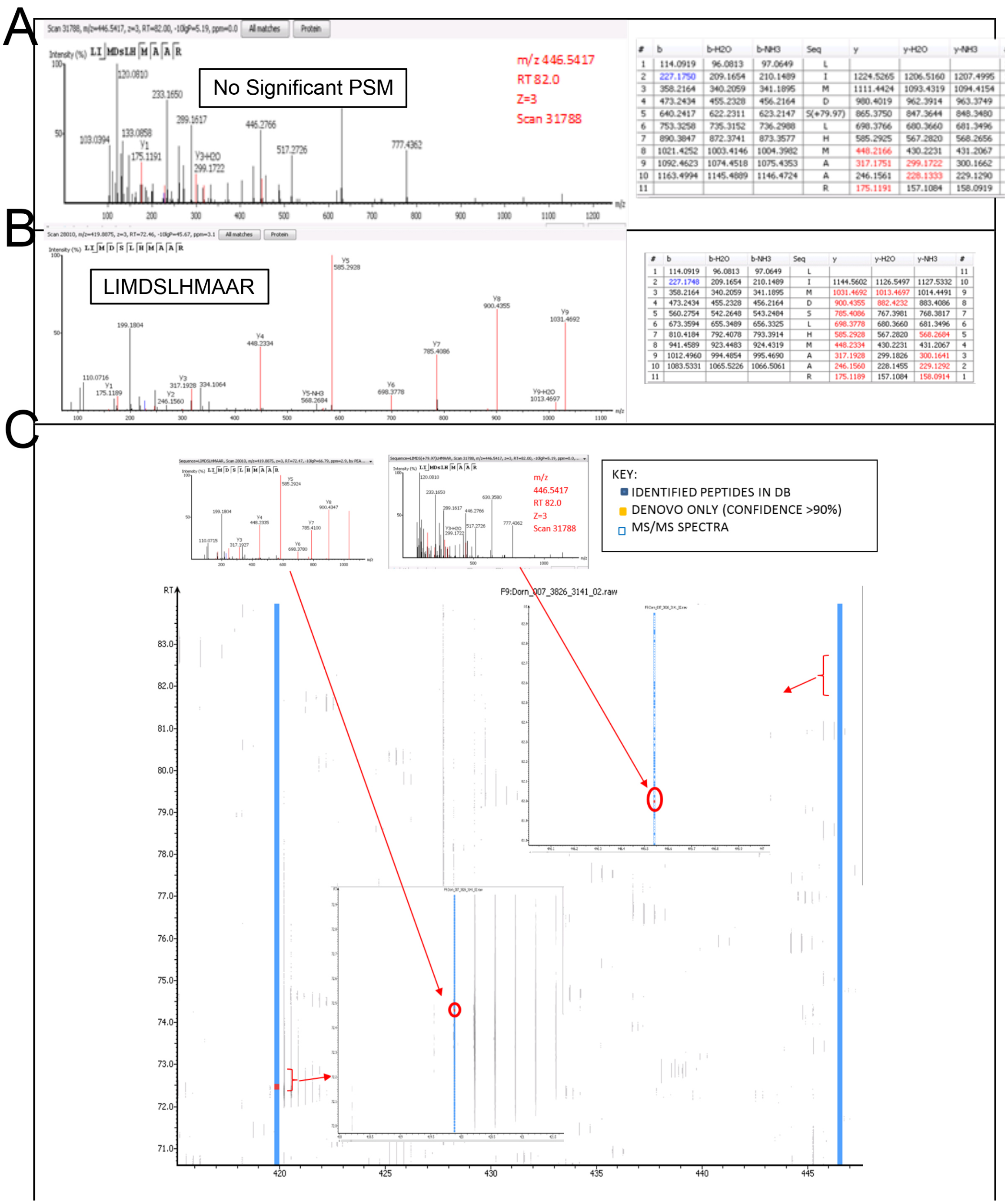

Fig. S9. *High-resolution tandem mass spectra of peptides from tryptic digest of GRK-treated recombinant human Mfn2.* (A) Representative non-matching spectrum from the elution window of the Ser-378 phosphopeptide. (B) Matching spectrum for the non-phosphorylated peptide from the GRK tryptic digest. The m/z values for the assigned ions are highlighted in the adjacent ion tables. (C) Retention time/m/z coordinates of tandem spectra that were analyzed by targeted LC-MS for phosphorylation of the Ser-378 containing peptide. The seven tandem spectra that were acquired at retention times between 82-83 min at m/z = 446.542 showed no evidence of phosphorylation.

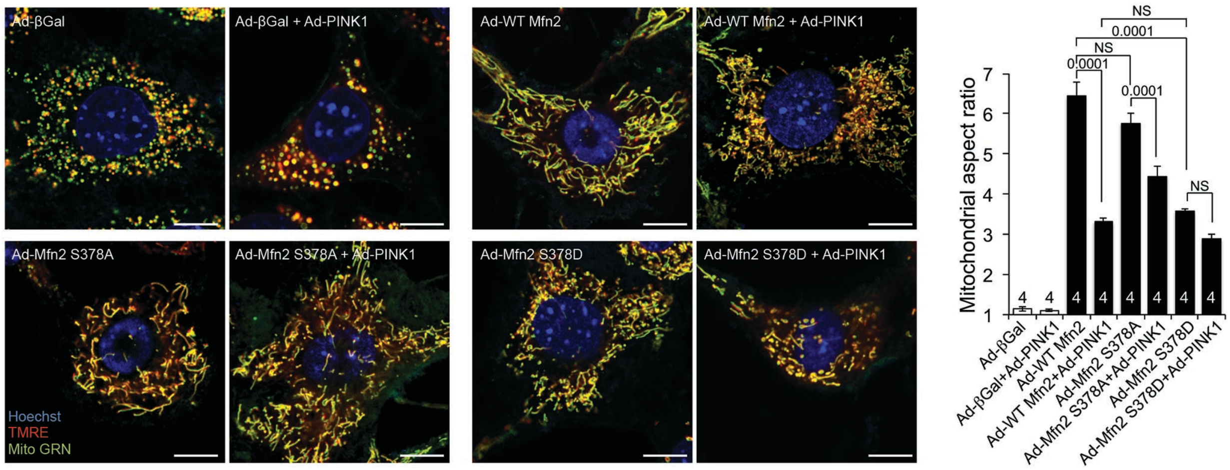

Fig. S10. *Representative live-cell confocal images from studies described in Figure 1H.* Mitochondria of Mfn1-/-, Mfn2-/- double knockout MEFs infected with adenoviri expressing Mfn2 mutants with or without adeno-PINK1 kinase were co-stained with MitoTracker Green (green) and TMRE (red); nuclei are stained blue with Hoechst. Scale bars are 10 μm. Quantitative group mean data to the right are reproduced from Figure 1H for comparison.

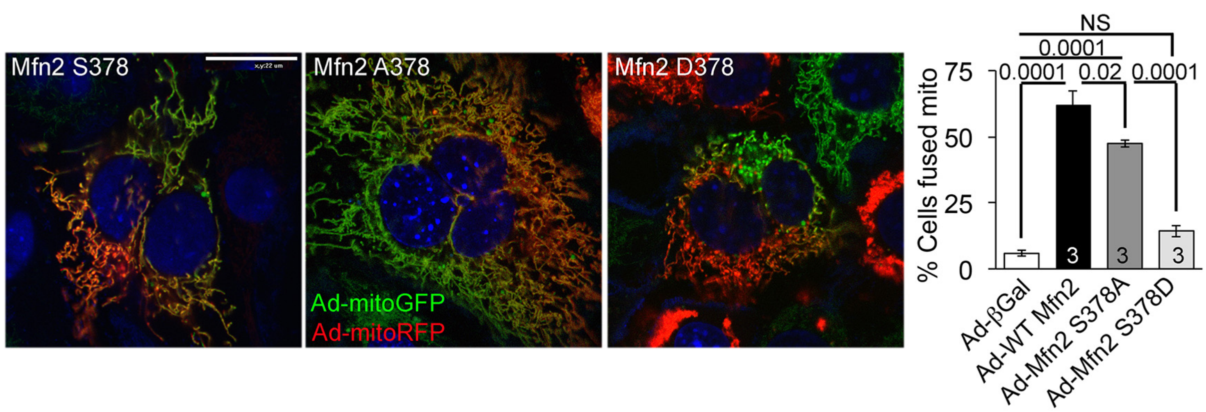

Fig. S11. *Effects of Mfn2 mutations that prevent or mimic Ser378 phosphorylation on mitochondrial fusion measured as content exchange.* **(left)** Representative live cell confocal images showing mitochondrial fusion (red/green mixing) 3 hours after PEG treatment of Mfn1-/-, Mfn2-/- double knockout MEFs expressing Mfn2 Ser378 mutants. Scale bar is 21 μm. N=3 independent studies; p values are by ANOVA with Tukey's post hoc comparison.

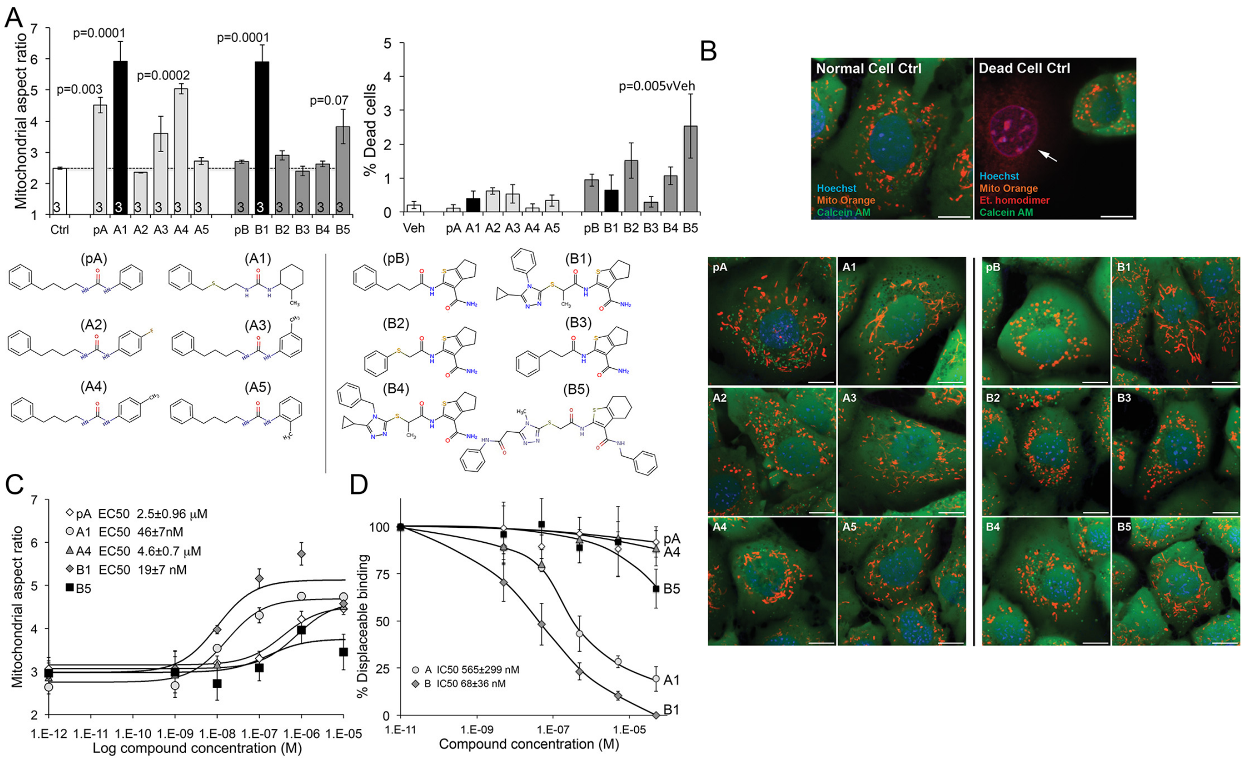

Fig. S12. *Small molecule mimetics of Mfn2 HR1 amino acid side chains that interact with HR2 are mitofusin agonists.* **(A)** Functional screening for class A and B small mitofusin agonists. 1μM of each candidate compound was added to Mfn2-deficient MEFs overnight. Mitochondrial aspect ratio is on left and cell viability on right. Structures of the class A and B chemosimilars are shown below (n=3; p values are by ANOVA with Tukey's post hoc comparison). Black bars indicate class A and B compounds selected for detailed studies. **(B)** Representative confocal images from studies in (A). Mitochondria were visualized with MitoTracker Orange. Cell viability was assessed simultaneously with mitochondrial aspect ratio - live cells have green cytoplasm (calcein AM) and dead cells lack calcein staining and have purple nuclei (red ethidium homodimer overlying blue Hoechst). Scale bars are 10 μm. **(C)** Initial dose-response relations of five fusogenic compounds from screening in (A). EC_{50} values (indexed to the 100% maximal response elicited by the most effective compound, B1) are shown for the agonists with strong fusion-promoting activity; mean±SEM of 3 independent studies for each compound. **(D)** Competition of the HR1 minipeptide at its Mfn2 HR2 binding site by five fusogenic compounds from (A). IC_{50} values are shown for agonists with >50% displacement (mean±SEM of 6 independent experiments per compound). Displacement curves for compounds A and B are re-plotted in Figure 2C.

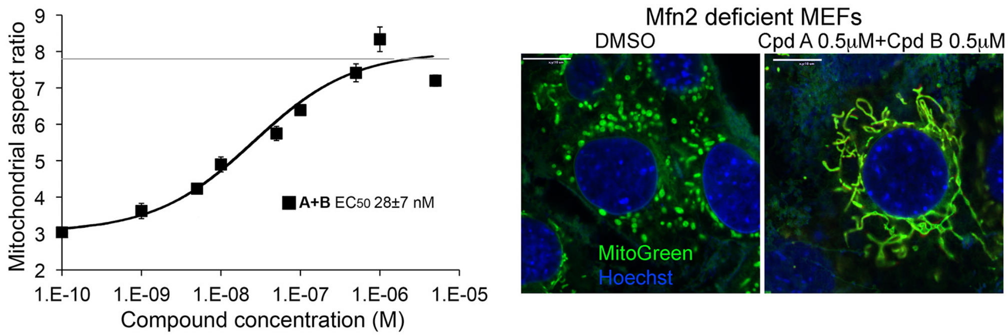

Fig. S13. *Synergistic effects of a class A and class B mitofusin agonist.* Mitochondrial elongation (increase in aspect ratio) in Mfn2-/- MEFs stimulated by equimolar concentrations of mitofusin agonists A and B. Dose-response curve on the left is from 6 independent experiments. Peak aspect ratio achieved with A+B is ~25% greater than with either agonist alone (compare to fig.12C). Representative live-cell confocal images are on right. Scale bar is 10 μm.

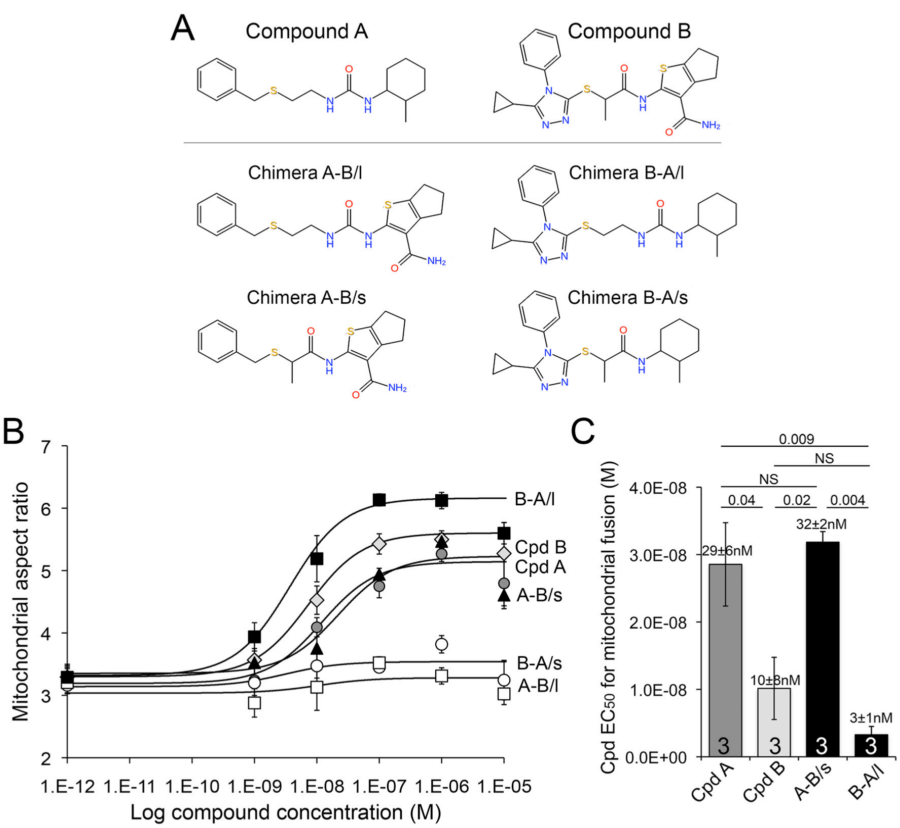

Fig. S14. *Evaluation of chimeric small molecule mitofusin agonists.* **(A)** Structures of compounds A and B and their chimeras. **(B)** Dose-response of compounds in (A) to promote mitochondrial fusion (increase in aspect ratio) in Mfn2-/- MEFs. Data for compounds A and B and chimera B-A/l in Figure 2B are re-plotted here for comparison. **(C)** Comparison of EC50 values calculated from studies in panel B. p values are from ANOVA with Tukey's test.

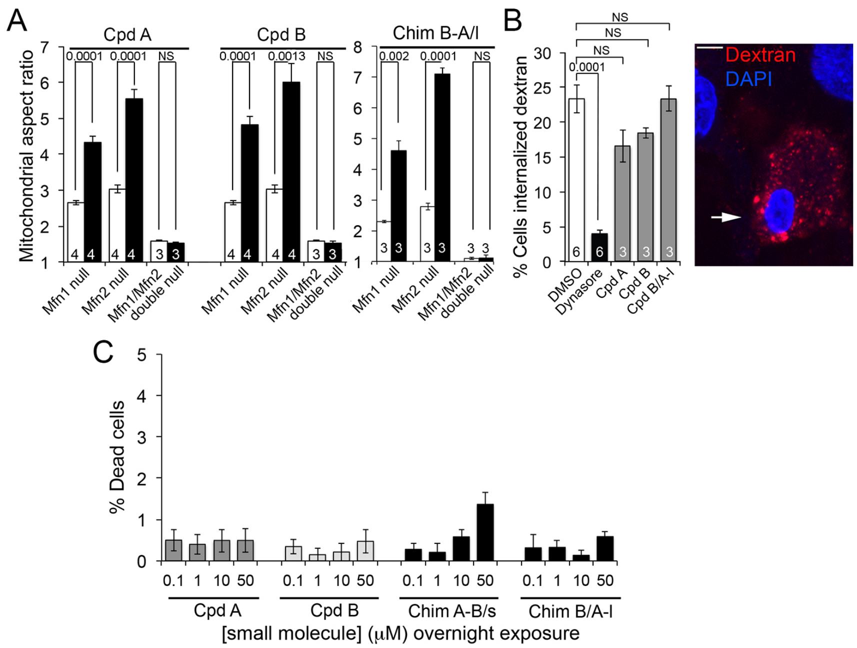

Fig. S15. *Functional evaluation of structurally diverse mitofusin agonists.*
(A) Mitochondrial elongation stimulated by mitofusin agonists A and B or chimera B-A/l in cells having different Mfn expression profiles. White bars are vehicle (DMSO) treated, black bars are 1 μM agonist overnight; * = p<0.05 vs vehicle (t-test). **(B)** Effects of cpds A and B or chimera B-A/l (1μM) on dynamin-mediated endocytosis of Alexa-Fluor 594 Dextran. Dynasore is a dynamin inhibitor. **(C)** Cell viability assessed after overnight exposure to indicated concentrations of mitofusin agonist (n=4). Test compounds were not uniformly soluble at concentrations greater than 50 μM. p values are by ANOVA with Tukey's test.

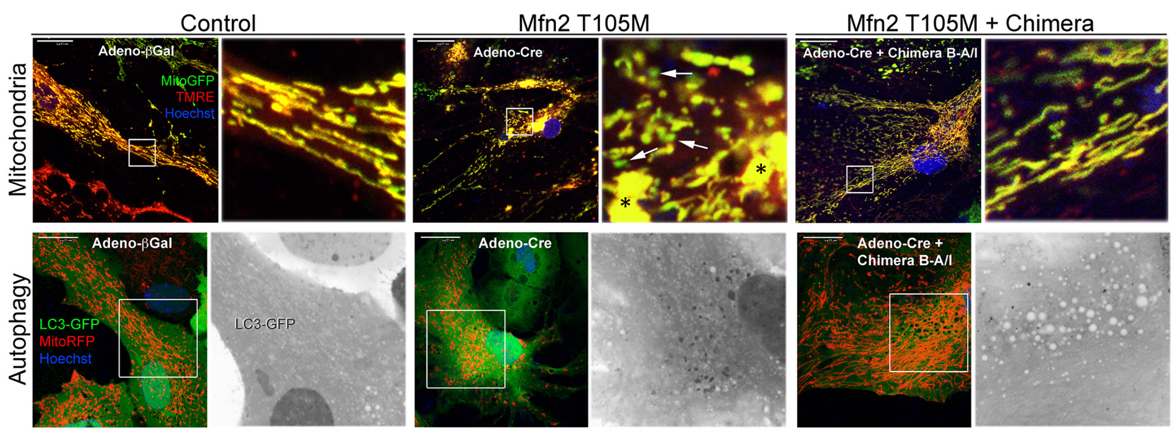

Fig. S16. *Mitofusin agonist chimera B-A/l reverses mitochondrial abnormalities induced by CMT2A mutant Mfn2 T105M in cultured mouse neurons.* Representative confocal images of living mouse neurons expressing MitoGFP and stained with TMRE and Hoescht from experiments reported in Figures 4B and 4C. Scale bars are 21 μm; expanded views are from white squares. Mfn2 T105M expression from the flox-stop transgene was induced by addition of adeno-Cre.

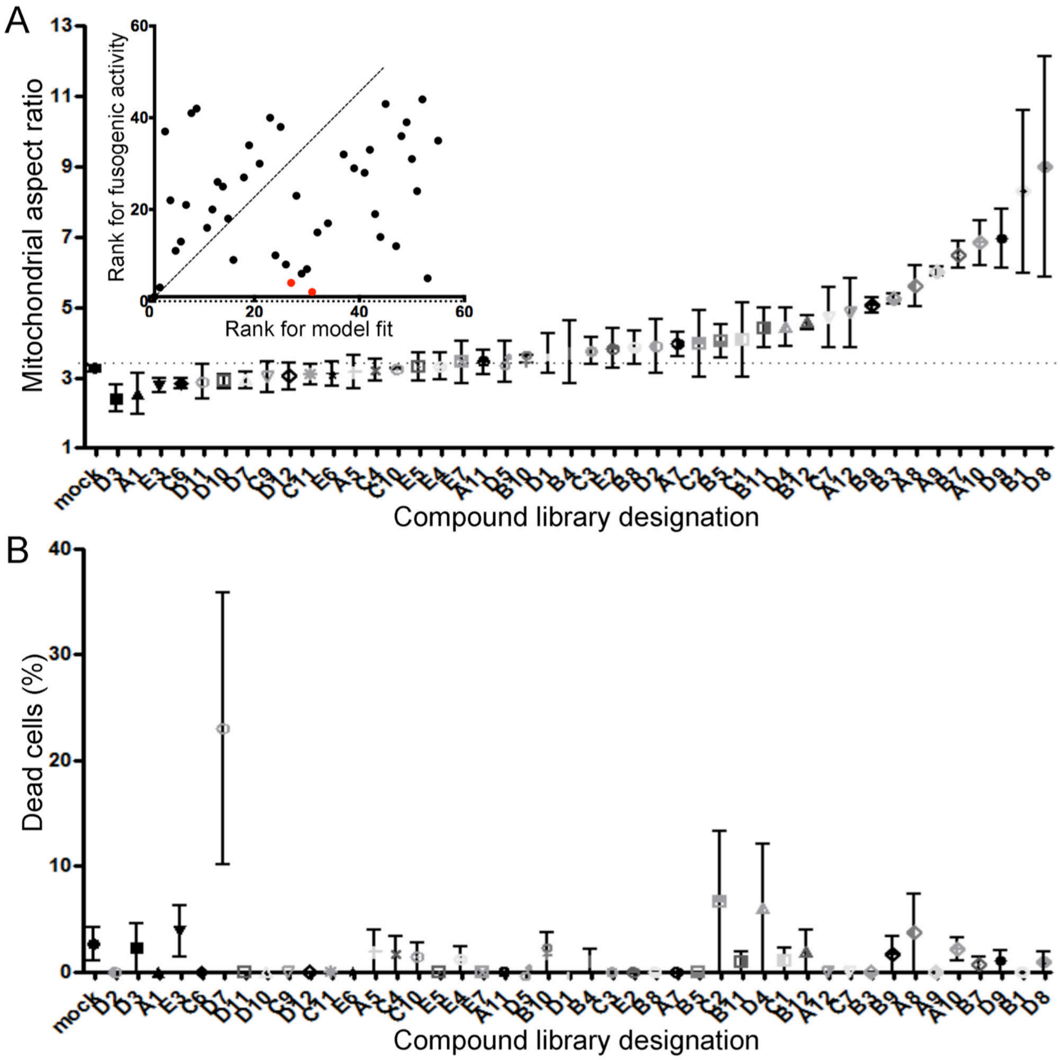

Fig. S17. *Functional screening for fusogenic activity of mitofusin agonist pharmacophores.*
A. Mitochondrial fusogenicity measured as aspect ratio of Mfn2 null MEFs after overnight treatment with 1 μM indicated library compound. Chemical details, structures, and commercial sources of these compounds are in **Supplemental dataset 2**. Mock = DMSO vehicle control. Horizontal dotted line indicates baseline value. Cells treated with 5 μM mitofusin agonist peptide HR1 367-384 (positive control) had aspect ratios of ~6. *Inset*: correlation of rank order for initial model fit vs actual fusogenicity (r=0.214). Red dots are compounds A10 and B1 that ranked 4^{th} and 2^{nd} for fusogenicity, but 22^{nd} and 31^{st}, respectively, for fit to the original pharmacophore model. **B.** Cytotoxicity measured by live-dead assay. Compounds are ranked by fusogenicity as in A. Means±SEM of 3 independent experiments examining ~30 cells per experiment.

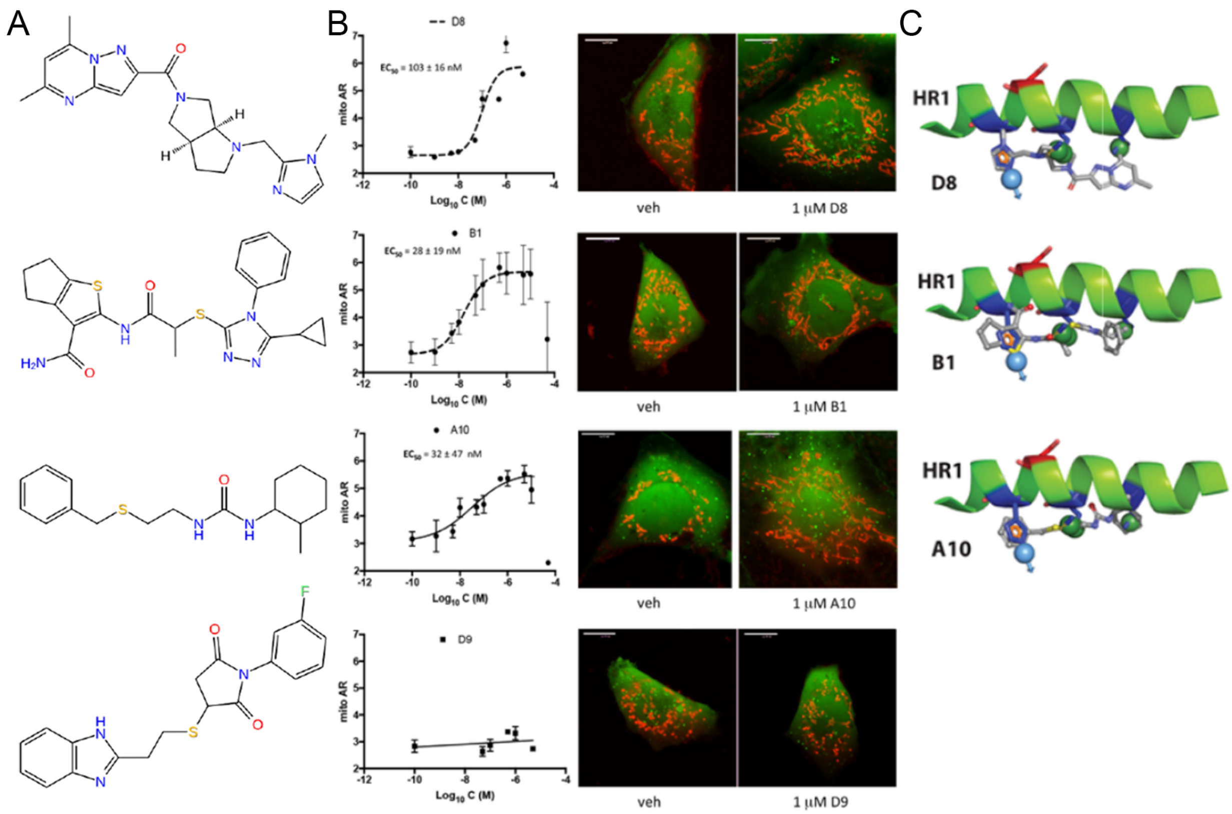

Fig. S18. *Functional validation and dose-response relations of candidate fusogenic small molecules.* **A.** Chemical structures of 4 top candidate fusogenic compounds from initial screening (see Fig. S17). **B.** Dose relations with representative images of vehicle and 1 μM treated Mfn2 null MEFs for each of the compounds, only 3 of which were true positives. Cells are stained with Mitotracker orange, calcein AM (green; alive) and ethidium homodimer (red nucleus; dead). There are no dead cells. EC_{50} values are provided for true positives; D9 showed no true fusogenic activity. Scale bars are 10 microns. Dose-response curves are means±SEM of 3 independent experiments. **C.** Schematic depiction of pharmacophore model fit for the 3 true positive fusogenic compounds.

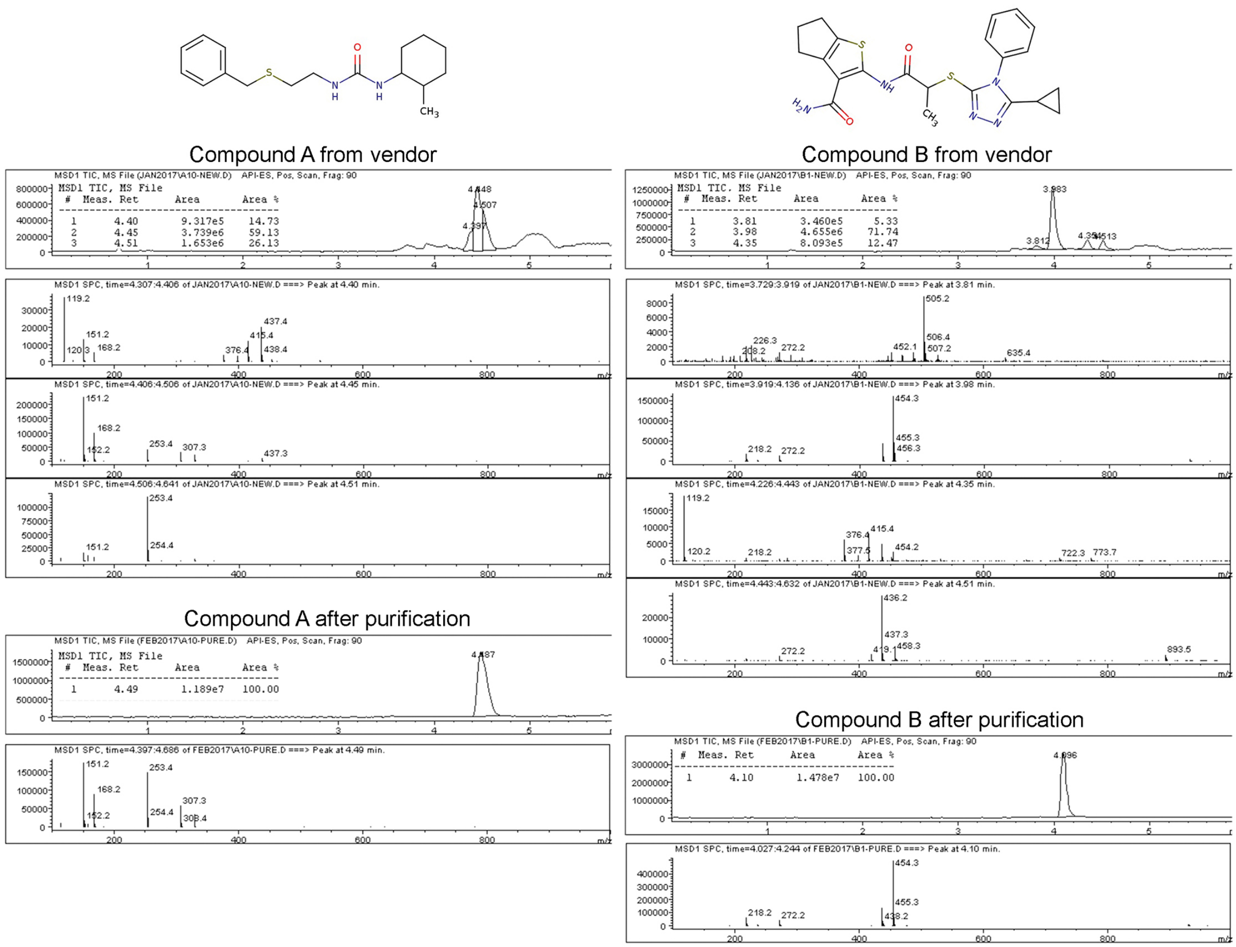

Fig. S19. *Purification of mitofusin agonist compounds A and B.* At the top are high performance liquid chromatography and mass spectra of compounds as they were obtained from the commercial vendor. On the bottom are spectra after in-house purification. Cpd A: expected m/z 306.18, exact mass found 307.3 $[M + H]^+$; Cpd B: expected m/z 453.15, exact mass found 454.3 $[M + H]^+$.

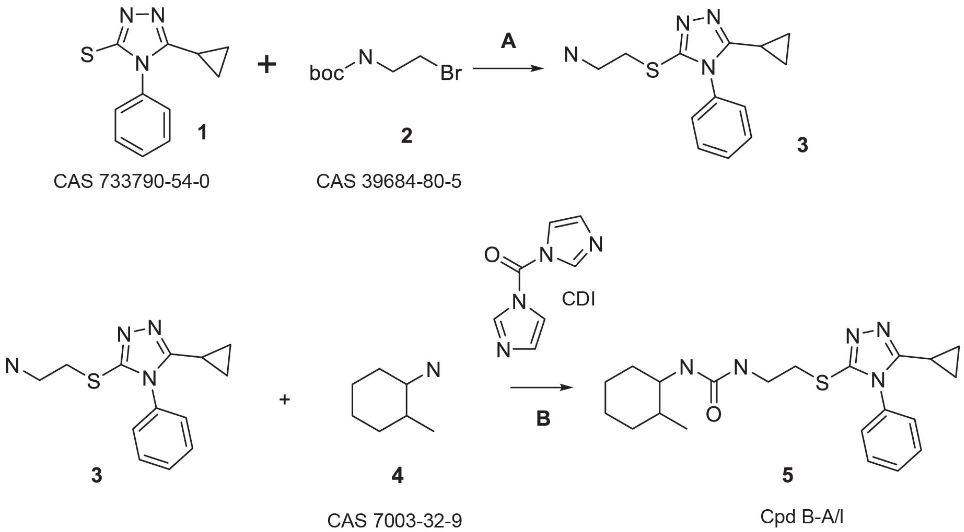

Fig. S20. *Synthetic route for preparation of Chimera B-A/l (compound 5).*

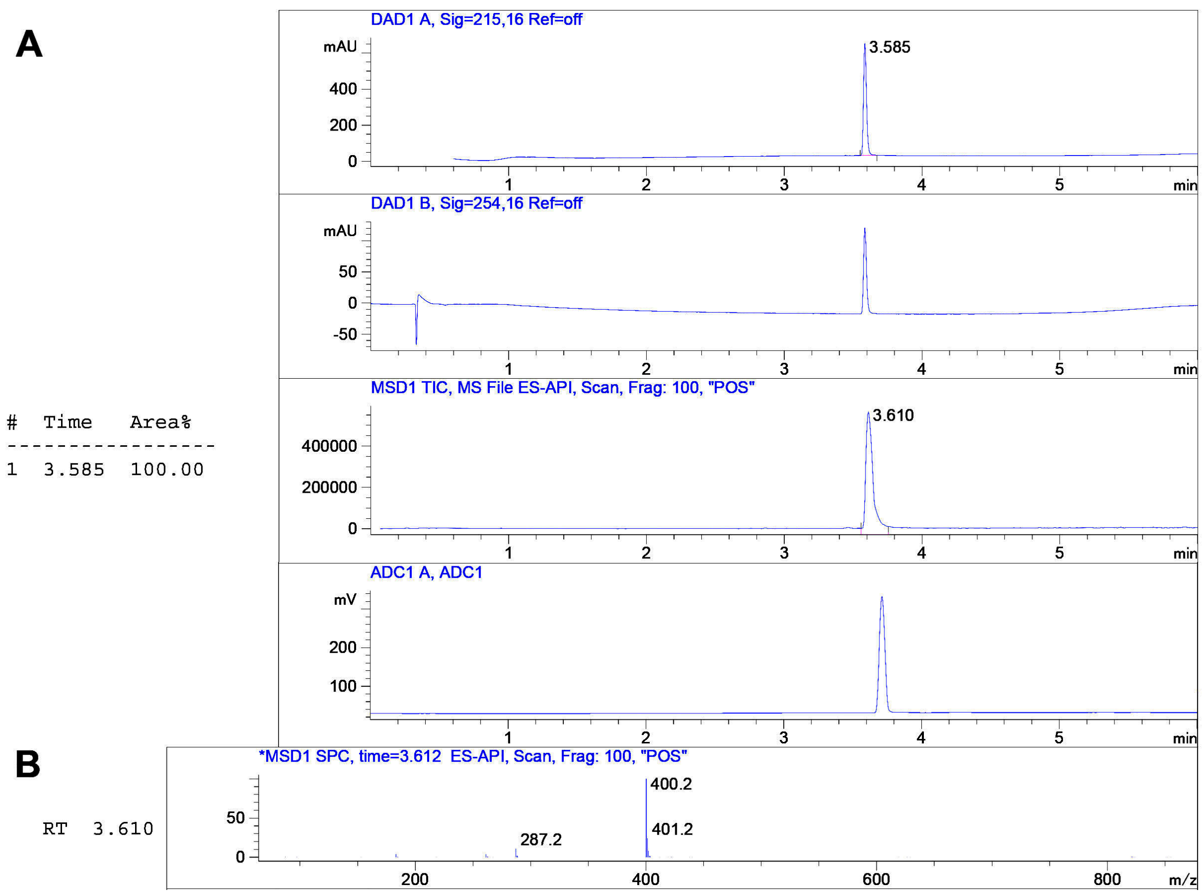

Fig. S21: *RP-HPLC and HRMS of newly synthesized chimera B-A/l.* **(A)** HPLC spectrum of chimera B-A/l. From top to bottom: UV Absorbance at 215nm; UV Absorbance at 254nm; complete ionization mass selective detector (MSD) spectrum; evaporative light scattering detection spectrum. Chimera B-A/l was 99.99% pure. **(B)** HRMS chromatogram of compound B-A/l (C21H29N5OS) shows exact mass: $[M + H]^+$: 400.2.

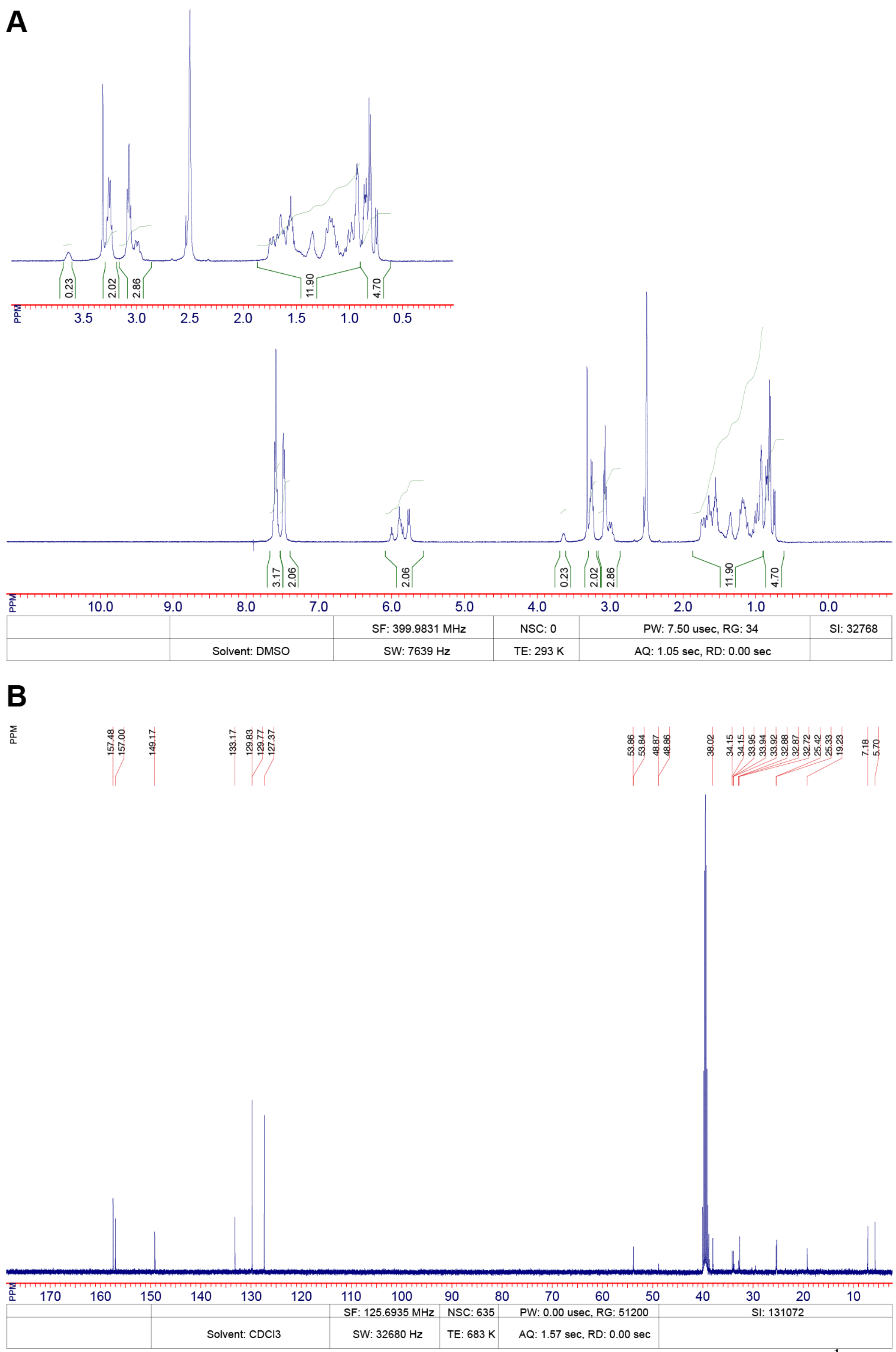

Fig. S22: *Proton and carbon-13 NMR of newly synthesized chimera B-A/l.* **(A)** Full ^{1}H NMR spectrum (400 MHz) of compound B-A/l (DMSO-d_6 solvent) and expanded view of region δ 0.0 – 4.0 PPM. **(B)** ^{13}C NMR spectrum (126 MHz) of compound B-A/l ($CDCl_3$ solvent).

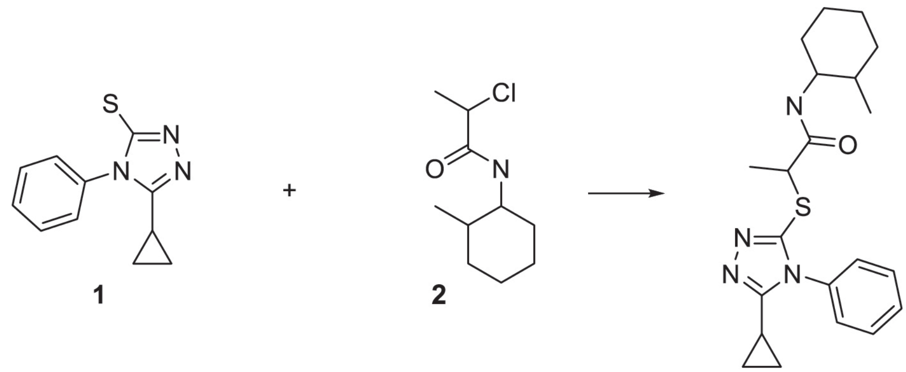

1 2 3

CAS 733790-54-0 CAS 923206-07-9 Cpd B-A/s

Fig. S23. *Synthetic route for preparation of chimera B-A/s (compound 3).*

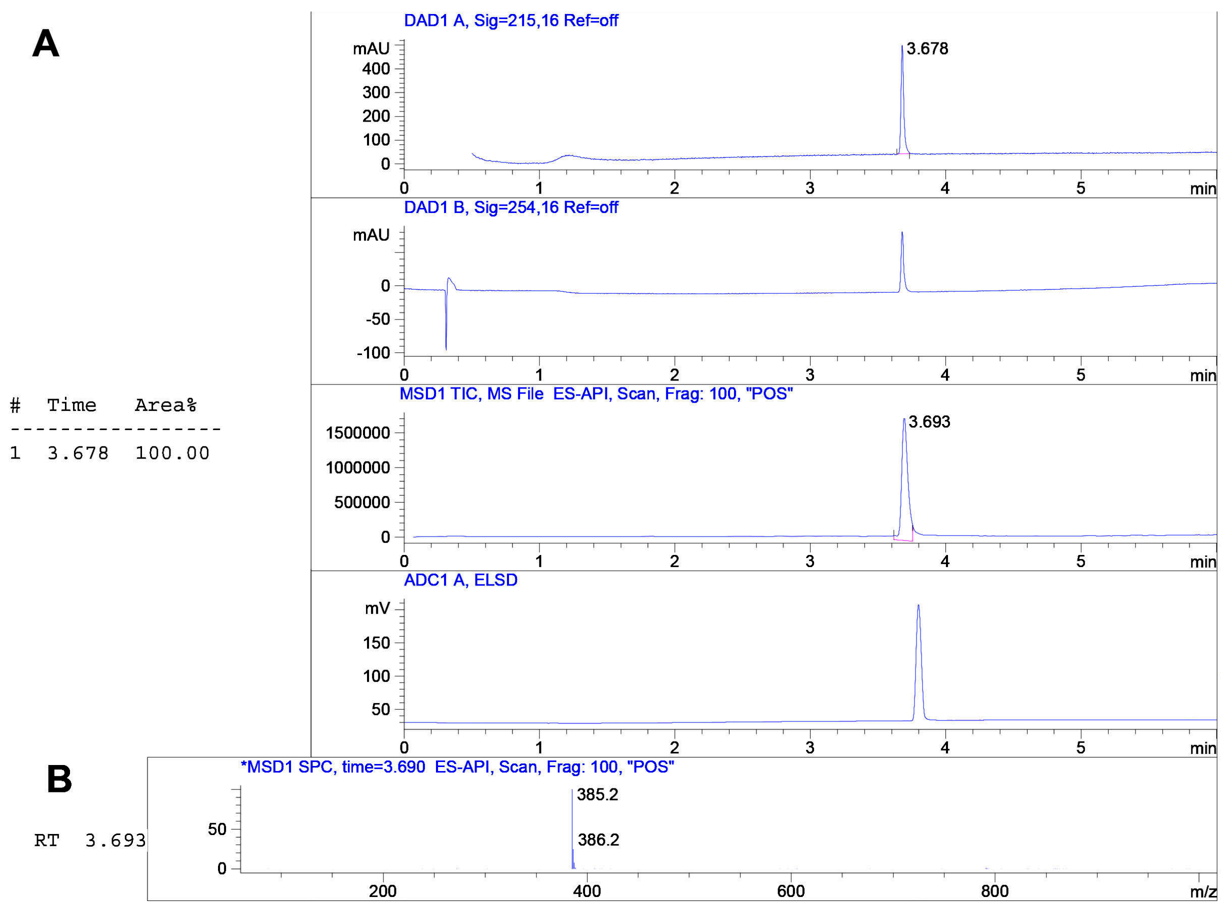

Fig. S24: *RP-HPLC and HRMS of newly synthesized chimera B-A/s.* **(A)** HPLC spectrum of compound B-A/s. From top to bottom: UV Absorbance at 215nm; UV Absorbance at 254nm; complete ionization MSD spectrum; evaporative light scattering detection spectrum. Chimera B-A/s was 99.99% pure. **(B)** HRMS chromatogram of compound B-A/s (C21H28N4OS) shows exact mass found: $[M + H]^+$: 385.2.

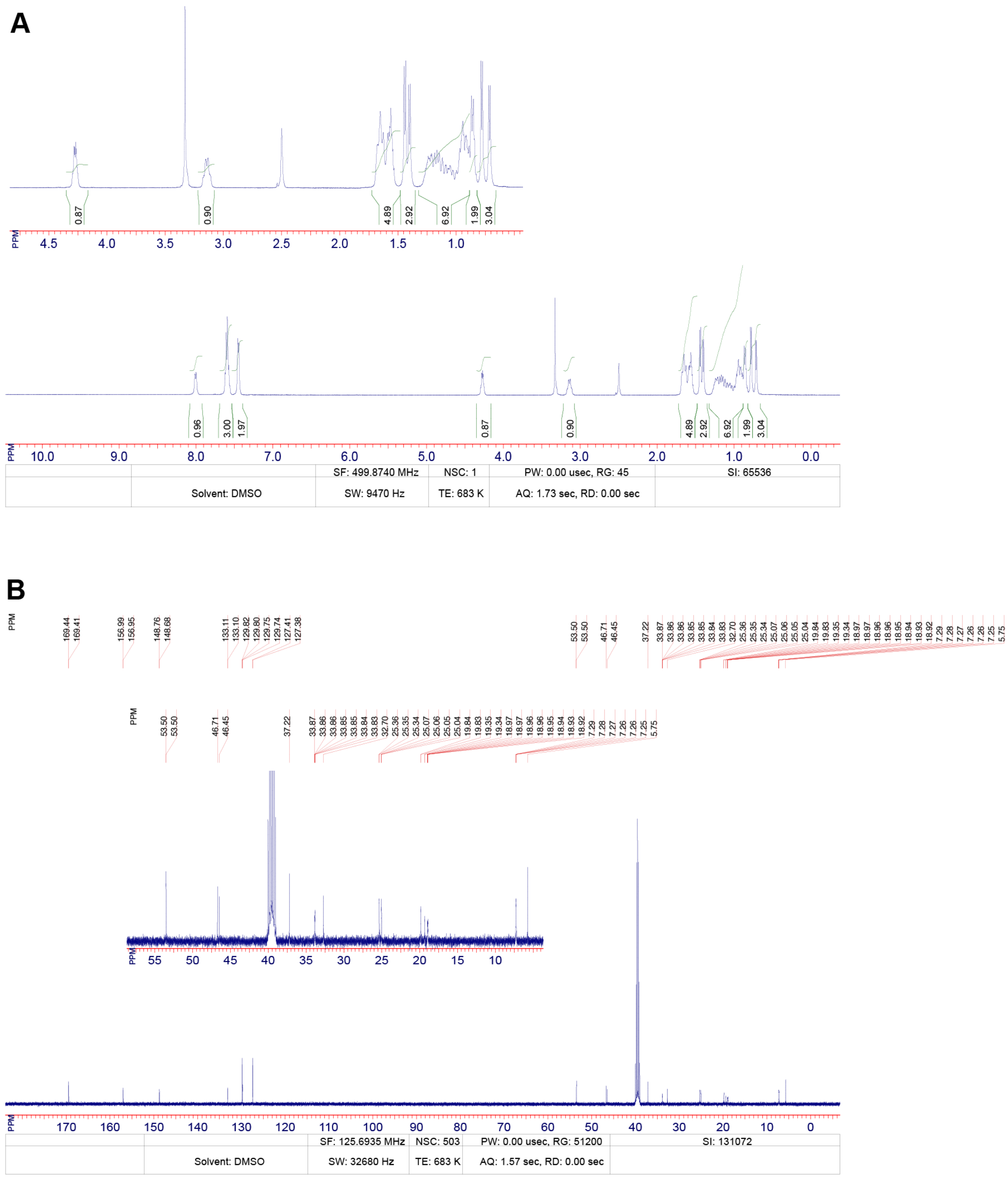

Fig. S25: *Proton and carbon-13 NMR of newly synthesized chimera B-A/s.* **(A)** Full ^{1}H NMR spectrum (500 MHz) of compound B-A/s (DMSO-d_6 solvent) and expanded view of region δ0.5 – 4.8 PPM. **(B)** ^{13}C NMR spectrum (126 MHz) of compound B-A/s (DMSO-d_6 solvent) and expanded view of region δ 5 – 60 PPM.

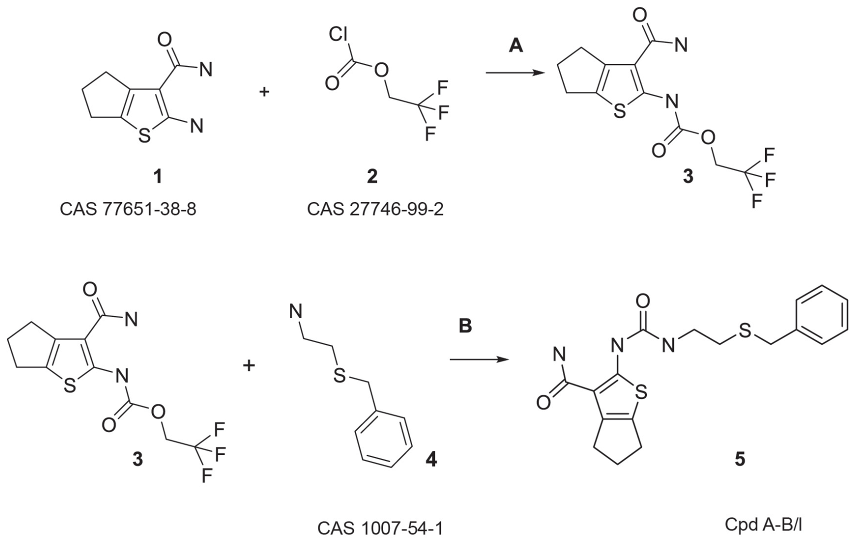

Fig. S26. *Synthetic route for preparation of chimera A-B/l (compound 5).*

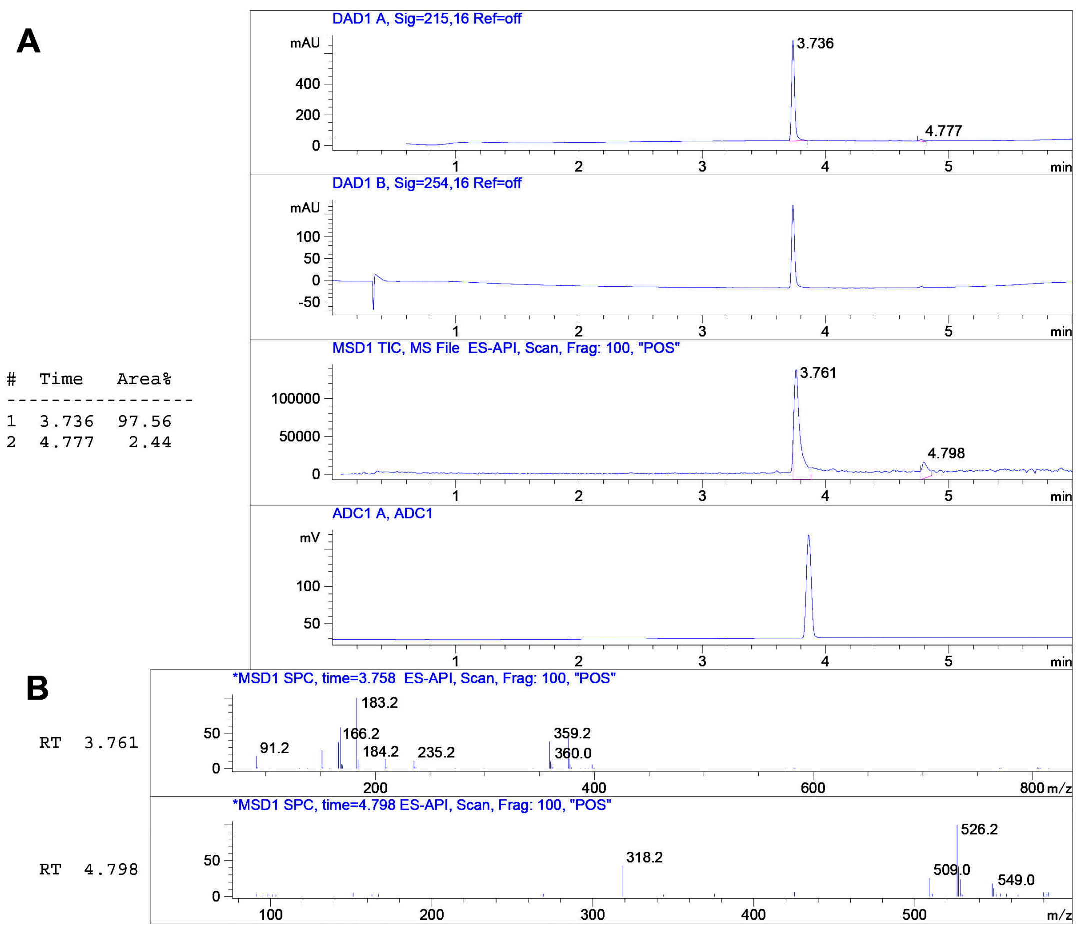

Fig. S27: *RP-HPLC and HRMS of newly synthesized chimera A-B/l.* **(A)** HPLC spectrum of newly synthesized chimera A-B/l. From top to bottom: UV Absorbance at 215nm; UV Absorbance at 254nm; complete ionization MSD spectrum; evaporative light scattering detection spectrum. Chimera A-B/l was 97.56% pure. **(B)** HRMS chromatogram of compound A-B/l (C18H21N3O2S2) shows exact mass found: $[M + H]^+$: 376.0.

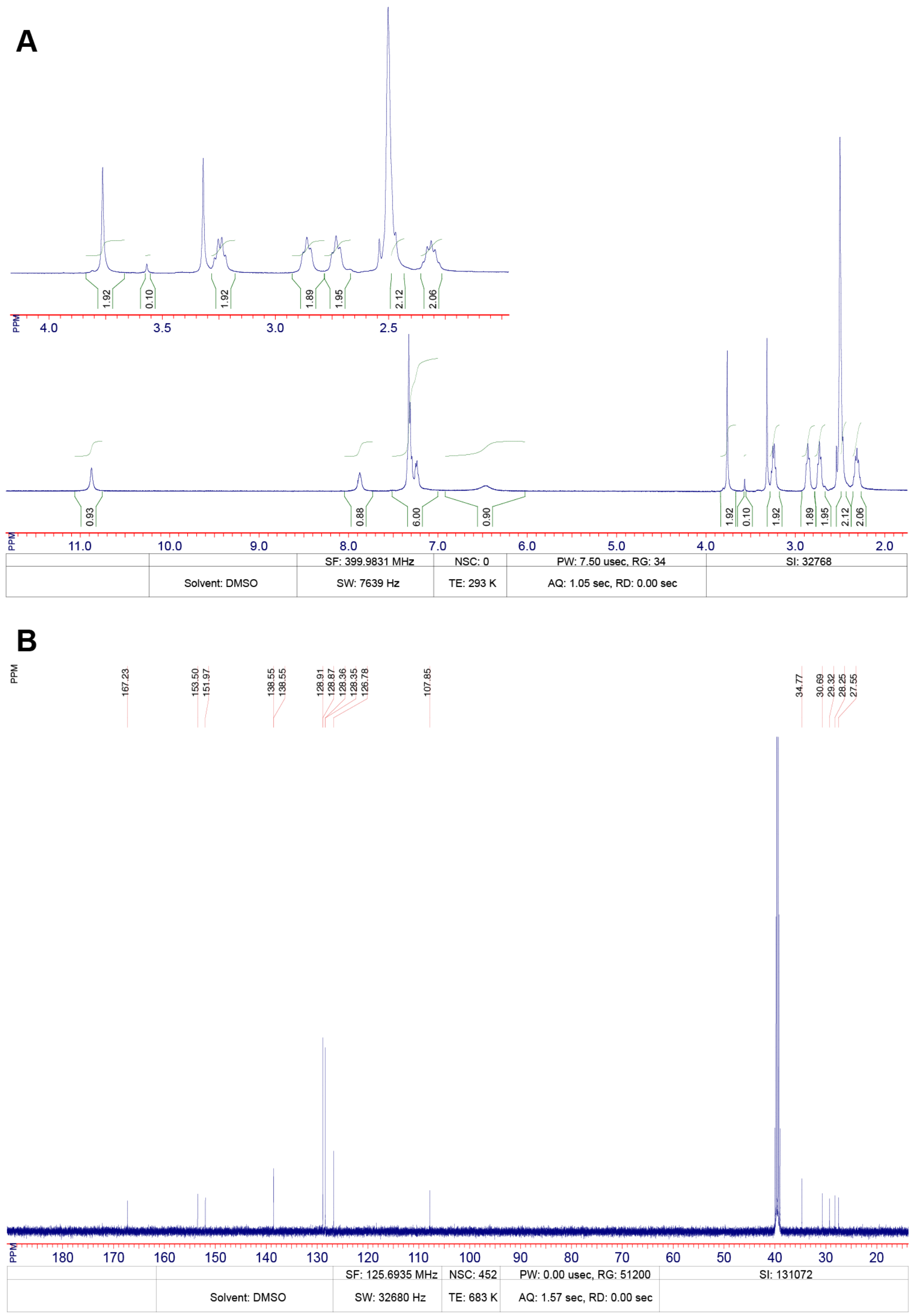

Fig. S28: *Proton and carbon-13 NMR of newly synthesized chimera A-B/l.* **(A)** Full ^{1}H NMR spectrum (400 MHz) of newly synthesized chimera A-B/l (DMSO-d_6 solvent) and expanded view of region δ 2.0 – 4.1 PPM. **(B)** ^{13}C NMR spectrum (126 MHz) of chimera A-B/l (DMSO solvent).

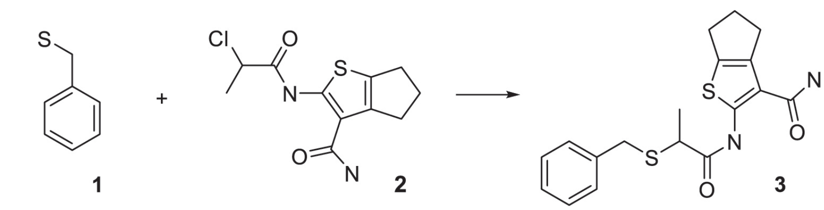

Fig. S29. *Synthetic route for preparation of chimera A-B/s (compound 3).*

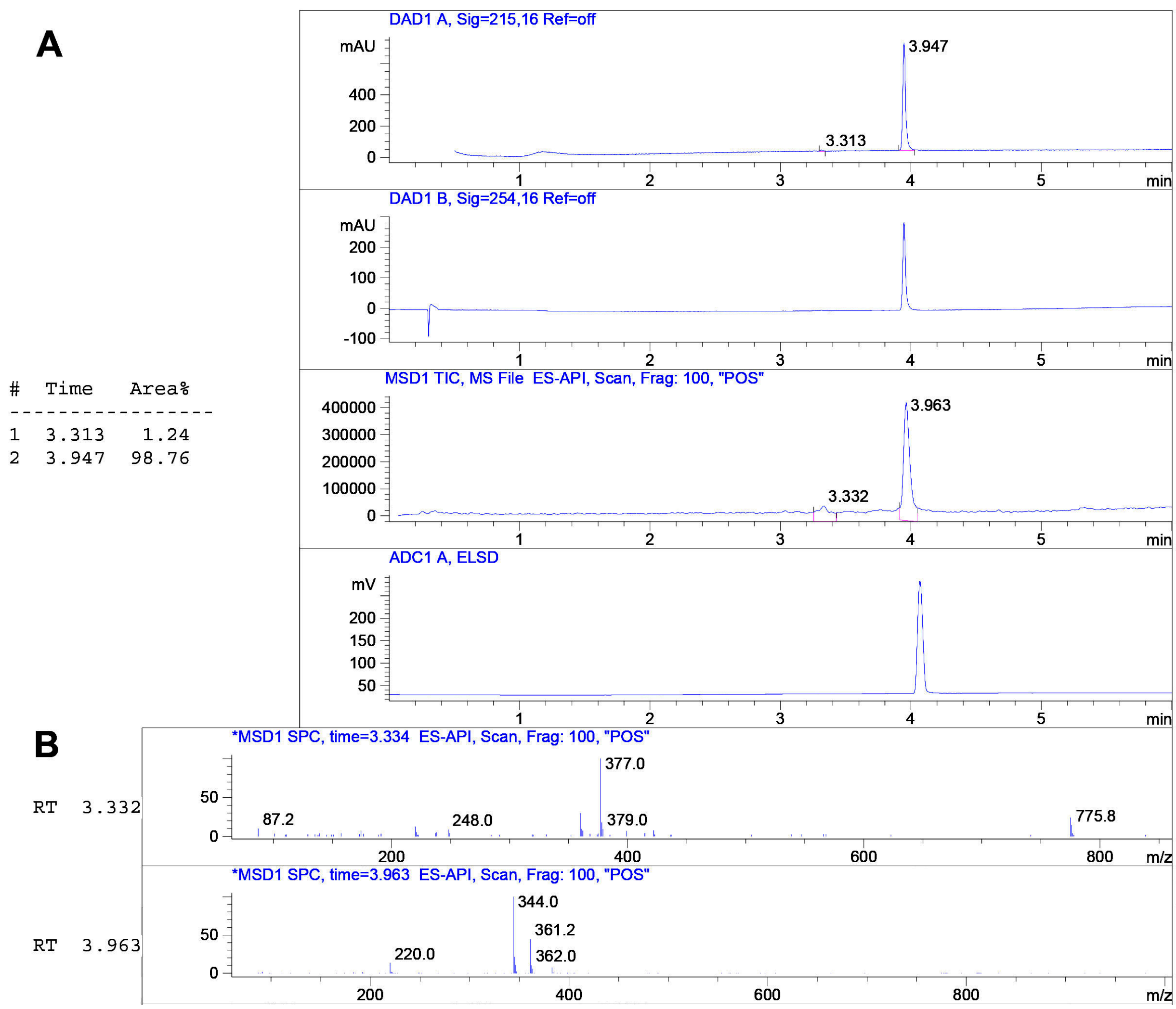

Fig. S30: *RP-HPLC and HRMS of newly synthesized chimera A-B/s.* **(A)** HPLC spectrum of compound A-B/s. From top to bottom: UV Absorbance at 215nm; UV Absorbance at 254nm; complete ionization MSD spectrum; evaporative light scattering detection spectrum. Chimera A-B/s was 98.76% pure. **(B)** HRMS chromatogram of chimera A-B/s (C18H20N2O2S2) shows exact mass found: $[M + H]^+$: 361.2.

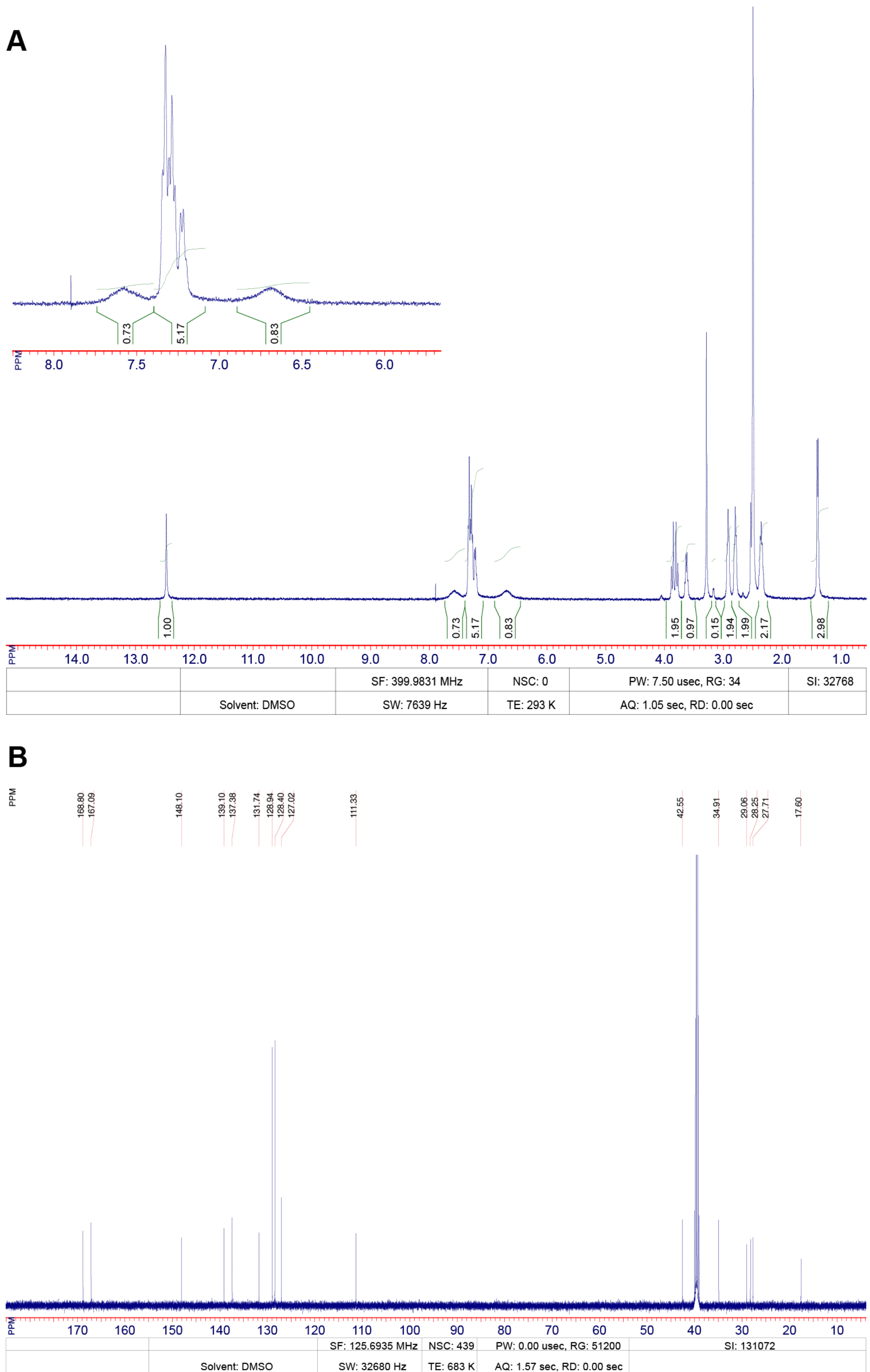

Fig. S31: *Proton and carbon-13 NMR of newly synthesized chimera A-B/s.* **(A)** Full ^{1}H NMR spectrum (400 MHz) of chimera A-B/s (DMSO-d_6 solvent) and expanded view of region δ 5.7 – 8.2 PPM. **(B)** ^{13}C NMR spectrum (126 MHz) of chimera A-B/s (DMSO-d_6 solvent).

Supplemental Table S1. *Fragmentation ions from tandem MS of Mfn phosphopeptides*

LIMDsLHMAAR[1] (*m/z*=446.543)

ion	*m/z* (Theoretical)	m/z (Observed)	ppm
y_1	175.119	175.120	3.7
y_3	317.193	317.194	1.4
y_4	448.234	448.230	-9.0
y_5	585.293	585.290	-3.6
y_6	698.377	698.380	5.0
y_7-$H_3PO_4^{+2}$	384.203^{+2}	384.203	0.7
y_8-H_3PO_4	882.425	882.427	2.3

LIMDsLHMAAR-[$^{13}C_6$][$^{15}N_4$] (*m/z*=449.880)

ion	*m/z* (Theoretical)	*m/z* (Observed)	ppm
y_1	185.127	185.127	0.2
y_2	256.164	256.163	-4.3
y_3	327.201	327.200	-3.1
y_4	458.242	458.242	-0.7
y_5	595.301	595.300	-1.0
y_6	708.385	708.382	-4.6
y_7-H_3PO_4	777.406	777.404	-3.7
y_8-H_3PO_4	892.433	892.431	-2.1
y_9-H_3PO_4	1023.474	1023.472	-1.7
y_{10}-H_3PO_4	1136.558	1136.549	-8.0

[1] The lower case single amino acid abbreviation indicates the phosphorylated residue.